Paleoproterozoic arc basalt–boninite–high magnesian andesite–Nb enriched basalt association from the Malangtoli volcanic suite, Singhbhum Craton, eastern India: Geochemical record…

Article · November 2016

DOI: 10.1016/j.jseaes.2016.09.015

CITATIONS
15

READS
682

7 authors, including:

Mutum Rajanikanta Singh
Wadia Institute of Himalayan Geology
18 PUBLICATIONS **229** CITATIONS
SEE PROFILE

Prof. Dr. C. Manikyamba
National Geophysical Research Institute
114 PUBLICATIONS **2,381** CITATIONS
SEE PROFILE

Sohini Ganguly
Goa University
50 PUBLICATIONS **590** CITATIONS
SEE PROFILE

Jyotisankar Ray
University of Calcutta
67 PUBLICATIONS **375** CITATIONS
SEE PROFILE

Journal of Asian Earth Sciences 134 (2017) 191–206

Contents lists available at ScienceDirect

Journal of Asian Earth Sciences

journal homepage: www.elsevier.com/locate/jseaes

Full length Article

Paleoproterozoic arc basalt-boninite-high magnesian andesite-Nb enriched basalt association from the Malangtoli volcanic suite, Singhbhum Craton, eastern India: Geochemical record for subduction initiation to arc maturation continuum

M. Rajanikanta Singh [a], C. Manikyamba [a,*], Sohini Ganguly [b], Jyotisankar Ray [c], M. Santosh [d,e], Th. Dhanakumar Singh [a], B. Chandan Kumar [f]

[a] National Geophysical Research Institute (Council of Scientific and Industrial Research), Uppal Road, Hyderabad 500 007, India
[b] Department of Earth Science, Goa University, Taleigao Plateau, Goa 403206, India
[c] Department of Geology, University of Calcutta, 35, B.C. Road, Kolkata 700 019, India
[d] School of Earth Science and Resources, China University of Geosciences, Beijing, China
[e] Centre for Tectonics, Resources and Exploration, Department of Earth Sciences, University of Adelaide, SA 5005, Australia
[f] Department of Geology, Central University of Kerala, Kasaragod 671316, Kerala, India

ARTICLE INFO

Article history:
Received 12 March 2016
Received in revised form 9 September 2016
Accepted 21 September 2016
Available online 15 November 2016

Keywords:
Singhbhum Craton
Malangtoli volcanic suite
Boninites
High Mg-andesites
Mantle wedge metasomatism

ABSTRACT

The Singhbhum Craton of eastern India preserves distinct signatures of ultramafic-mafic-intermediate-felsic magmatism of diverse geodynamic affiliations spanning from Paleo-Mesoarchean to Proterozoic. Here we investigate the 2.25 Ga Malangtoli volcanic rocks that are predominantly clinopyroxene- and plagioclase-phyric, calc-alkaline in nature, display basalt-basaltic andesite compositions, and preserve geochemical signatures of subduction zone magmatism. Major, trace and rare earth element characteristics classify the Malangtoli volcanic rocks as arc basalts, boninites, high magnesian andesites (HMA) and Nb enriched basalts (NEB). The typical LILE enriched-HFSE depleted geochemical attributes of the arc basalts corroborate a subduction-related origin. The boninitic rocks have high Mg# (0.8), MgO (>25 wt.%), Ni and Cr contents, high Al_2O_3/TiO_2 (>20), Zr/Hf and $(La/Sm)_N$ (>1) ratios with low $(Gd/Yb)_N$ (<1) ratio, TiO_2, and Zr concentrations. The HMA samples are marked by moderate SiO_2 (>54 wt.%), MgO (>6 wt.%), Mg# (0.47) with elevated Cr, Co, Ni and Th contents, depleted $(Nb/Th)_N$, $(Nb/La)_N$, high $(Th/La)_N$ and La/Yb (<9) ratio, moderate depletion in HREE and Y with low Sr/Y. The NEBs have higher Nb contents (6.3–24 ppm), lower magnitude of negative Nb anomalies with high $(Nb/Th)_{pm}$ = 0.28–0.59 and $(Nb/La)_{pm}$ = 0.40–0.69 and Nb/U = 2.8–34.4 compared to normal arc basalts [Nb = <2 ppm; $(Nb/Th)_{pm}$ = 0.10–1.19; $(Nb/La)_{pm}$ 0.17–0.99 and Nb/U = 2.2–44 respectively] and HMA. Arc basalts and boninites are interpreted to be the products of juvenile subduction processes involving shallow level partial melting of mantle wedge under hydrous conditions triggered by slab-dehydrated fluid flux. The HMA resulted through partial melting of mantle wedge metasomatized by slab-dehydrated fluids and sediments during the intermediate stage of subduction. Slab-melting and mantle wedge hybridization processes at matured stages of subduction account for the generation of NEB. Thus, the arc basalt-boninite-HMA-NEB association from Malangtoli volcanic suite in Singhbhum Craton preserves the signature of a complete spectrum of Paleoproterozoic active convergent margin processes spanning from subduction initiation to arc maturation.

1. Introduction

The convergent plate margins are potential sites of effective cycling of materials and energy through interaction between surface and deep earth processes, ocean-crust-mantle interactions, delamination and recycling of oceanic crust in the mantle, generation of juvenile continental crust and mineral deposits (Tatsumi, 2005; Iwamori and Nakamura, 2015; Santosh et al., 2015; Yang et al., 2016). The geochemical exchange of elements between the subducted oceanic slab and sub-arc mantle wedge, the different stages of subduction from initiation to maturation and associated

* Corresponding author.
E-mail address: cmaningri@gmail.com (C. Manikyamba).

http://dx.doi.org/10.1016/j.jseaes.2016.09.015
1367-9120/

melt generation processes, interaction between subduction-derived magmas and overlying arc crust, and subduction-driven asthenospheric upwelling collectively account for the diverse compositional spectra of magmas produced through subduction zone processes. Geochemical signature of subduction zone magmas is one of the most viable tools to understand subduction processes, elemental cycling and chemical variability controlled by tectonic pulses (Perfit et al., 1980; Hawkesworth et al., 1993; Spandler and Pirard, 2013).

During the course of subduction, from initiation to maturation, the mantle wedge is chemically modified and enriched by the influx of hydrous fluids released by the dehydration of the down-going oceanic crust, siliceous slab melts derived by melting of subducted slab and subduction-derived sediments (Kimura and Yoshida, 2006; van Keken et al., 2011; Mullen and McCullum, 2014) which in turn serve as the most viable agents for transfer of different elements from slab to mantle wedge (Stern et al., 1990; Elburg et al., 2002; Elliott et al., 1997). These subduction-derived components eventually trigger metasomatism and flux-controlled partial melting of mantle wedge (McCulloch and Gamble, 1991; Elliott et al., 1997; Elburg et al., 2002; Polat and Kerrich, 2006; Li et al., 2013; Shuto et al., 2013; Sato et al., 2013; Kimura and Nakajima, 2014; Liu et al., 2015). Arc magmas including tholeiitic to calc-alkaline basalts, basalt-andesite-dacite-rhyolite (BADR) associations, boninites, picrites, siliceous high-Mg basalts (SHMB), adakites, high-Mg andesites (HMA) and Nb-enriched basalts (NEB) are influenced by relative contributions from subducted sediments, slab dehydrated fluids and melts of subducted basaltic oceanic crust, thereby signifying distinct episodes of magmatism at fore-arc, arc and back arc regimes consistent with different stages of subduction. Boninites are high Mg and high Si volcanic rocks with extremely depleted incompatible trace element (HREE; Nb, Ta, etc.) signatures with variable enrichment of LILE (Rb, Ba, K, etc.) formed either during subduction initiation or in hot subduction zones, marked by high Al_2O_3/TiO_2 ratios; U-shaped REE patterns with La/Sm > 1 but Gd/Yb < 1; negative Nb anomalies with Nb/La < primitive mantle value of <1.03; variable enrichment of Zr, Hf; high Mg#, Cr, Co and Ni contents relative to island arc tholeiites (Polat and Kerrich, 2006). However, basaltic magmas marked by distinct HFSE enrichment coupled with low LILE/HFSE and LREE/HFSE ratios, weakly positive or negative Nb anomalies and $(La/Nb)_N$ ratio varying between 0.7 and 2 have been reported from arc, rifted arc and back arc settings (Sajona et al., 1996; Wyman et al., 2000). Based on variations in HFSE abundances and subduction zone petrogenetic processes, the HFSE enriched magmas have been described as adakites, high magnesian andesites (HMA), high Nb basalts (HNB) and Nb enriched basalts (NEB; Hollings and Kerrich, 2000; Polat and Kerrich, 2001; Viruete et al., 2007; Wang et al., 2008; Hastie et al., 2011). According to Kelemen (1995), the HMA magmas were more common than basalts in the past compared to Cenozoic arcs due to selective preservation related to erosion and subduction zone processes. High-Mg andesites are spatially and temporally associated with boninites and adakites and these are generated either by melting of refractory mantle at low pressure (in association with boninites) or by the interaction of mantle peridotite with adakitic slab melts (Schuth et al., 2012). The NEBs are characterized by high Nb/La (>0.5), elevated abundances of HFSE and have an alkaline or transitional alkaline character (Kepezhinskas et al., 1996; Defant and Kepezhinskas, 2001; Petrone and Ferrari, 2008). The adakite-magnesian andesite-NEB assemblage occurring in association with "normal" tholeiitic to calc-alkaline subduction-derived magmas have been reported from few Archean greenstone belts of Superior Province, Canada, Greenland, Quebec, Baltic Shield and Western Australia; Gadwal and Penakacherla greenstone belts of Dharwar Craton, India; as well as from Cenozoic arcs of Mindanao and Zamboanga (Phillippines), Mexico, Panama, Ecuador (Central and South America), Qiangtang terrane (central Tibet), Xinjiang (northwest China), Alataw (western China), Aleutians, northern Kamchatka and Hispaniola (Caribbean islands) (Sajona et al., 1996; Hollings and Kerrich, 2000; Polat and Kerrich, 2001, 2006; Polat et al., 2002; Zhang et al., 2005; Wang et al., 2007, 2008; Viruete et al., 2007; Manikyamba and Kerrich, 2012; Manikyamba et al., 2005, 2008, 2009). It has been postulated that adakites, magnesian andesites, and NEB of Archean and Phanerozoic heritage represent shallow subduction of hot, young oceanic crust where melting of subducted slab generates adakites, hybridization of peridotitic mantle wedge by adakitic melts gives rise to magnesian andesites and NEB are produced by the melting of this hybridized residue (Defant and Drummond, 1990; Kepezhinskas et al., 1996; Polat and Kerrich, 2001; Hastie et al., 2011). Arc basalt-boninite and adakite-HMA-NEB associations, reflecting initial and matured stages of subduction respectively, have been documented from Archean greenstone terranes as well as from the ~43 Ma old Izu-Bonin-Mariana plate convergence systems. However, magmatic associations showing complete preservation of arc basalt-boninite-HMA-NEB compositions rarely occur in ancient cratons but are important for evaluating mantle processes and volcanic activity spanning from initial to matured stages of subduction processes during Precambrian.

The geological history of the Singhbhum Craton of eastern Indian shield is marked by spatial and temporal distribution of ul tramafic-mafic-intermediate-felsic magmatism. However, detailed geochemical studies have been conducted only in limited areas covering Dalma, Dhanjori, Jagannathpur and IOG (Saha, 1994; Bose, 2000; Mukhopadhyay, 2001; Misra and Johnson, 2005; Misra, 2006; Mukhopadhyay et al., 2012). Precise geochemical data to characterize the volcanic rocks present in the different formations and their tectonic discrimination are scanty. Earlier workers have documented petrographic and limited geochemical studies on the Malangtoli lavas covering limited area (Ray et al., 2006). Recent studies on the Paleo-Mesoarchean OMG volcanic rocks have documented the presence of boninites and island arc tholeiites endorsing the oldest subduction processes in the Singhbhum Craton (Manikyamba et al., 2015). In the present paper, we report for the first time island arc basalts, high Mg-andesites (HMA) and NEBs that are associated with boninitic volcanic rocks from the Paleoproterozoic Malangtoli volcanic suite of Singhbhum Craton, we address the geochemical features, petrogenesis and geodynamic setting of these rocks to place constraints on the Paleoproterozoic subduction zone processes of the Singhbhum Craton. Given the rarity of arc basalt-boninite-HMA-NEB association and the interesting magmatic and tectonic parameters controlling their genesis, our study has important implications in understanding Precambrian crustal evolution processes in the Singhbhum Craton.

2. Geological setting

The Singhbhum Craton of eastern India consists of distinct crustal blocks that preserve the signatures of several episodes of volcanism, sedimentation and metallogenic events spanning from Paleoarchean to Mesoproterozoic (Saha, 1994; Bose, 2000; Mukhopadhyay, 2001; Mazumder, 2005; Misra, 2006; Eriksson et al., 2006; Sharma, 2009; Mukhopadhyay et al., 2014). The oldest components of this craton are represented by granitoids and their enclaves that are considered as 'Singhbhum nucleus' which is surrounded by volcano-sedimentary associations and supracrustal sequences (Naqvi and Rogers, 1987; Saha, 1994; Weaver, 1990; Bose, 2009). The Precambrian granite-greenstone terranes of Singhbhum Craton (Fig. 1) are divided into (1) the Older Metamorphic Group (OMG), (2) Older Metamorphic Tonalite Gneiss

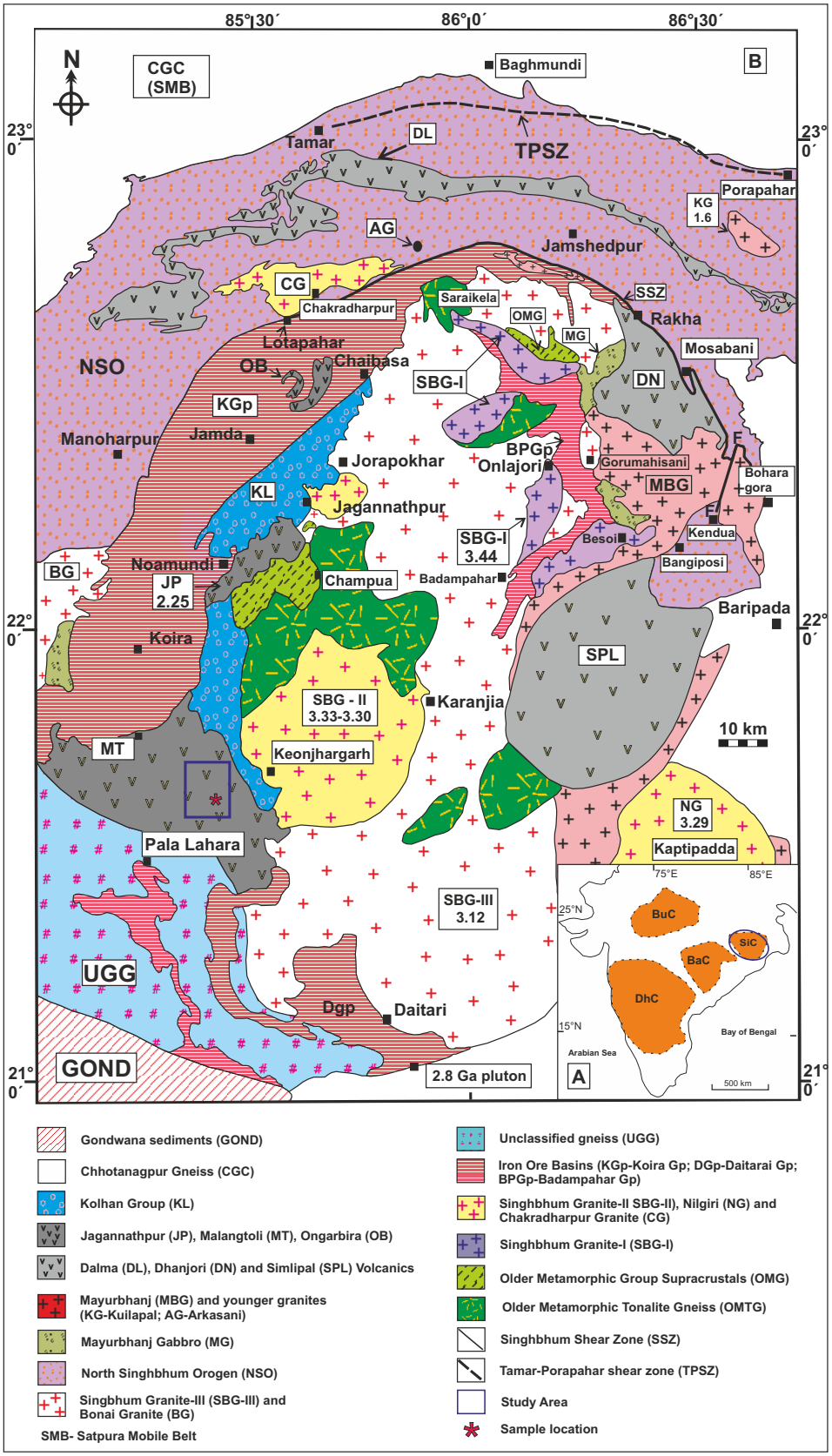

Fig. 1. (A) Inset map showing different cratons in the peninsular India (after Sharma, 2009). (B) Simplified geological map of Singhbhum Craton (after Saha, 1994 and Misra, 2006) with sample locations.

Table 1
Stratigraphy of the Singbhum-Orissa craton, Eastern India (after Saha et al., 1988; Misra, 2006).

Stratigraphic unit	Geological events	Major lithologies	Age (Ga)
Newer Dolerite dykes and sills- phase I, II and III	Intrusion of dykes and sills	Quartz dolerite	~2.0–1.0
Kolhan Group	Deposition of sediments	Phyllite, limestone, sandstone-conglomerate	~<2.25
Jagannathpur and Malangtoli lavas	Volcanic eruption	Basalt, basaltic andesite	~2.25
Dhanjori and Dalma volcanics, Tamperkola granite	Mafic volcanism and felsic plutonism	Ultramafic - mafic tuffs, basalts, quartzite-conglomerate High Mg - lavas, pyroclastic rocks, granite	~2.80
	Thermal metamorphism of OMG, OMTG, SBG-II and SBG-III		~3.07–3.05
Mayurbhanj Granite and Gabbro (MBG)	Coeval emplacement of MBG	Granite, gabbro, picrite, anorthosite	~3.09
Simlipal lavas and metasediments	Formation of volcano-sedimentary basin	Spillites, tuffs, quartzites	~>3.09
Singhbhum Group	Formation and deformation of supracrustals sedimentation and magmatism	Pelites, felsic volcanic, mafic sills	~3.12–3.09
	Thermal metamorphism of OMG due to SBG-III and Bonai granite emplacement		~3.16–3.10
SBG-III	Emplacement of SBG-III	Granodiorite, granite	~3.12
Bonai Granite	Plutonic emplacement	Granite, granodiorite	~3.16
	Metamorphism of OMG, OMTG and IOG rocks		~3.24–3.20
Iron Ore Group (IOG)	Formation, structural deformation (folding)and metamorphism of IOG rocks	Mafic and felsic lavas, tuffs, shales, BHJ, BHQ, quartzite dolomite, conglomerate	~3.30–3.16
	Thermal metamorphism of OMG and OMTG due to SBG-II and Nilgiri granite emplacement		~3.30
Nilgiri Granite	Emplacement of Nilgiri Granite	Tonalite, Granite	~3.29
SBG-II	Emplacement of SBG-II	Granodiorite	~3.33–3.30
Singhbhum Granite (SBG I)	Emplacement of granitoid plutons	Tonalite, Granodiorite	~3.44–3.38
Older Metamorphic Tonalite Gneiss (OMTG)	Folding of OMG supracrustals and synkinematic intrusion of tonalite	Tonalite gneiss, granodiorite	~3.44–3.42
Older Metamorphic Group (OMG)	Deposition of sediments with mafic volcanism and plutonism	Pelitic schists, banded calc-gneiss, amphibolites	~3.55–3.44
Unstable sialic crust		Sialic sediments	3.6–3.55

(OMTG), (3) older granite-greenstone belts containing banded iron formation (BIF) of the Gorumahisani-Badampahar-Daitari Iron Ore Group, (4) granite plutons, (5) two units of younger greenstone belts of Dhanjori-Simlipal Group, (6) younger granites and (7) mafic dyke swarms (Newer Dolerite dykes; Mohanty, 2012). The tectonostratigraphic elements of Singhbhum Craton are summarized in Table 1. The OMG represents the oldest supracrustal assemblage of the Singhbhum Craton and comprises pelitic schists, quartz-magnetite-cumingtonite schists, quartzites, banded calc-gneiss, and para and ortho amphibolites reflecting the first cycle of mafic volcanism, plutonism and sediment deposition in the Singhbhum Craton. The volcano-sedimentary sequences of Iron Ore Group indicate second cycle of volcanism and sedimentation in the Singhbhum Craton (Saha et al., 1988; Saha, 1994; Misra, 2006; Mukhopadhyay et al., 2012; Mondal, 2009). The volcano-sedimentary sequences of Simlipal basin are coeval with the third cycle of magmatism and sedimentation of Singhbhum Craton. The Proterozoic north Singhbhum mobile belt got accreted along the northern margin of the Singhbhum platform (Bose, 2009). The Dalma and Dhanjori basins of the Proterozoic north Singhbhum mobile belt are distinctly marked by bimodal komatiite-tholeiite magmatism and sedimentary rocks. The ~2.25 Ga eruption of Jagannathpur and Malangtoli lavas post-dates the IOG mafic volcanism and are overlain by Kolhan Group of sediments which are followed by the emplacement of Soda Granite (~2.22 Ga) and Kuilapal Granite (~1.64 Ga; Saha, 1994; Saha et al., 1988; Bose, 2000; Misra, 2006). These granitoid intrusions, copper mineralization (~1.77–1.63 Ga) and associated shear zone activities along south Singhbhum shear zone (SSZ) were punctuated by different phases of intrusion of Newer Dolerite dyke with uranium mineralization along SSZ dated at ~1.58–1.48 Ga (Mohanty, 2012; Roy and Sarkar, 2006; Mazumder et al., 2010; Roy et al., 2002; Sarkar et al., 1986; Iyengar and Murthy, 1982; Sengupta et al., 1984). The intrusion of Newer Dolerite dyke phase III marked the final magmatic episode in the geological history of Singhbhum Craton (Misra and Johnson, 2005).

The Malangtoli volcanic rocks (Fig. 1) of Singhbhum Craton are exposed in an area of ~800 sq km covering Malangtoli in the north and Pala Lahara in the south (Saha, 1994; Ray et al., 2006). In the southern part, the Malangtoli lavas overlie an unconformity consisting of quartz-sandstone pebble beds designated as Mankharchua Group (Sarkar et al., 1986). At the eastern side, these volcanic rocks are overlain by the Kolhan Group sandstones and shales. To the west of Koenjhar, the Malangtoli volcanic rocks have a faulted contact with the BIFs of IOG (Ramakrishnan and Vaidyanadhan, 2010). In general, the Malangtoli volcanic rocks are predominantly mafic at some places but intermediate rocks are also identified recently from our field investigations. The mafic volcanic rocks are mostly massive in nature with sporadic occurrences of poorly preserved pillow structures. These pillows are highly sheared, deformed, chloritized and permeated by intense quartz and carbonate veins. These mafic rocks are associated with quartzites and conglomerates. It has been observed that the mafic lavas near Kanjipani area of Malangtoli are associated with quartzites, ironstones, conglomerates and talc schist (Banerjee et al., 2016) along with laterite as the cap rock.

The mineralogical composition of the studied samples is marked by pyroxenes and plagioclase occurring as essential minerals with opaque as accessory phases. Both clinopyroxene and plagioclase occur as phenocrysts and the groundmass is made of microphenocryst clinopyroxene, plagioclase and volcanic glass. Relict olivine is present in some samples. Plagioclase phenocrysts are saussuritized at some places and found in clusters within the groundmass showing glomeroporphyritic, vitrophyric and intersertal texture. Occasionally, tuffaceous fragments present in some sections are showing reaction rims with the surrounding magma resembling magmatic embayment. At some places, clinopyroxenes are altered to chlorite, fibrous amphibole, actinolite and tremolite

suggest greenschist facies metamorphism. Amphiboles are fractured, dismembered, sutured and have irregular grain boundaries. Opaques are iron oxides, mainly magnetite and chrome magnetite (Singh et al., 2016).

3. Sampling and analytical techniques

Relatively less weathered samples of boninites-arc basalt-HMA have been collected from the outcrops of recently excavated road on Kushakala and Banspal road (Fig. 2), whereas Nb enriched basalts belong to a canal cutting section at N21° 38′ 58.6″; E85° 20′ 59.1″. The samples are devoid of quartz-carbonate-sulphide veins and are distal to intrusive contacts and shear zones. After petrographic screening for altered mineralogy, 55 samples were analysed for major, trace and rare earth element concentration at CSIR-National Geophysical Research Institute, India. The rock samples were powdered to ~250 mesh in an agate mortar to avoid metal contamination. Major elements were analysed by XRF (Philips MAGIX PRO Modal 2440) using press pellets; relative standard deviation are within 5% and totals including with LOI (loss on ignition) were all 100 ± 1 wt.%. Trace elements including REE were determined by HR-ICP-MS (Nu Instruments, ATTOM High Resolution ICP-MS, UK), following the procedure of closed vessel acid digestion technique. 50 mg rock sample powder were dissolved in savillex vessels containing 10 ml acid mixture of HF:HNO_3 in 7:3 ratio, and kept on hot plate at 150 °C for 48 h. After complete digestion, 2–3 drops of perchloric acid ($HClO_4$) was added and the entire mixture was evaporated to complete dryness. Freshly

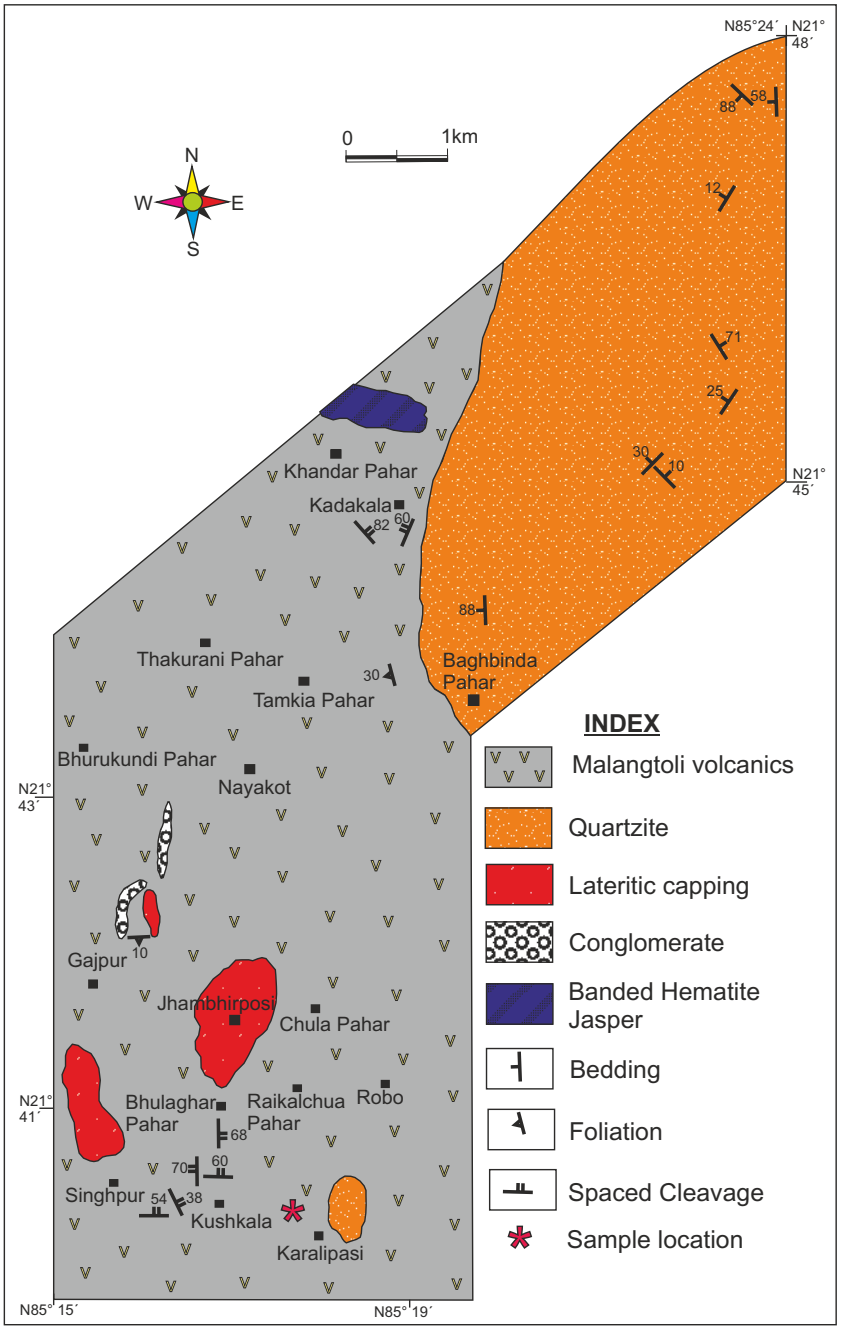

Fig. 2. Detailed geological map of Malangtoli region with sample locations of boninitic rocks along with arc basalts and high Mg andesites near Kushakala (after Banerjee et al., 2016).

prepared 20 ml of 1:1 HNO_3 was added and kept on hot plates at ~80 °C for 10–15 min. In the clear solution, 5 ml of Rh (1 ppm concentration) was added as an internal standard and made into 250 ml. 5 ml of this solution was further diluted to 50 ml to achieve suitable TDS (total dissolved solids). BHVO-1, JB-2 and JA-1 were run as standard reference materials during the analysis for monitoring the accuracy of the data. All the prepared solutions, blank and reference standards were introduced into HR-ICPMS through standard Meinhard® nebulizer with a cyclonic spray chamber housed in Peltier cooling system. The quantitative measurements were performed using the instrument software (Attolab v.1), while the data processing was done using Nu Quant®, which uses knowledge-driven routines in combination with numerical calculations (quantitative analysis) to perform an automated/manual interpretation of the spectrum of interest. External drift was corrected by repeated analyses of BHVO-1, JB-2 and JA-1, which were also used as calibration standards accordingly. Precision and reproducibility obtained for international reference materials BHVO-1, JB-2 and JA-1 given in Table S1 which are found to be better than 2% RSD for the majority of the trace elements.

4. Geochemical characteristics

Based on their geochemical compositions, the studied samples have been divided into high MgO basalts, basalts, Nb-enriched basalts (NEB) and high-Mg andesites (HMA; Table S2). These rocks

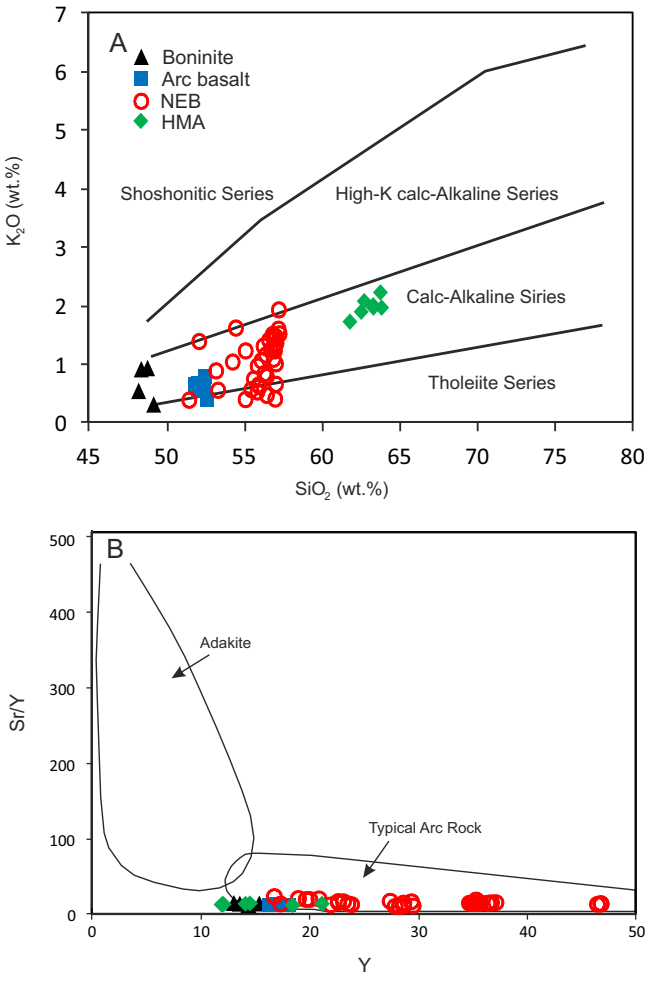

Fig. 3. (A) SiO_2 vs. K_2O discrimination figure in which Malangtoli lavas indicate medium to high K-calc-alkaline nature (Peccerillo and Taylor, 1976). (B) Island arc characteristics of Malangtoli volcanic suite (after Martin, 1986).

are predominantly calc-alkaline in nature with few of them occupying the field of tholeiites thereby attesting to typical arc signatures (Fig. 3A and B). The high MgO basalts have a restricted range of MgO (~27.5 wt.%) and SiO_2 (~44 wt.%) with low TiO_2 (0.3 wt.%), high Mg# (0.80), Cr (1237–1594 ppm), Ni (107–144 ppm) contents (Table S2). The total alkali content is very low compared with the associated basalts (1.55–2.07 wt.%). The higher Al_2O_3/TiO_2 (28) ratios compared with the chondrite value (20) reflect their boninitic nature. The associated basalts have a restricted range of SiO_2 (~48 wt.%) with lower MgO (9–10 wt.%), Mg# (0.52), relatively higher TiO_2 (0.82–0.85 wt.%), low Cr (335–368 ppm) and Ni (125–159 ppm), and slightly higher total alkalies (2.5–3.5 wt.%) in comparison with the high MgO varieties (Table S2). These high and low MgO basalts occupy the fields of boninite and arc tholeiites respectively on the Yb_N vs. Dy_N and Zr vs. Ti discrimination plots (Fig. 4). Further, in terms of Zr vs. Ti variations, the arc tholeiite samples reflect distinct MORB signatures (Fig. 4C). In terms of Yb vs. Ti relationship (Fig. 4B), the boninitic composition of the high MgO basalts is analogous with their Phanerozoic counterparts, whereas the arc basalts correspond to the field of Archean basalts, komatiites and Phanerozoic arc and oceanic basalts. The geochemical characteristics of calc-alkaline basalt samples (T 16, 17, 19, 21, 22, 23 and 25) marked by high SiO_2 (59–62 wt.%), MgO (7.1–7.7 wt.%), Mg# (~0.5) with elevated Cr (293–1173 ppm), Co (48–68 ppm), Ni (6–19 ppm) and Th (1.5–3.6 ppm) content classify them as high Mg andesites (HMA). The calc-alkaline basalts having slight enrichment in their SiO_2 (47–53 wt.%) with lower MgO (5.2–10.8 wt.%), Mg# (0.3–0.5), Cr (17–626 ppm), Ni (22–84 ppm) and elevated concentrations of Nb ranging from 6.3 to 24.7 ppm are classified as Nb-enriched basalts (NEB). The overall major and trace element attributes for the Nb enriched basalts are consistent with normal arc basalts except for the distinct enrichment in their Nb contents (6.3–24.6 ppm). Few analysed samples with >20 ppm Nb content can be categorized as high Nb basalts (HNB; Table S2). In terms of HFSE and REE chemistry, these rocks distinctly correspond to the field of NEB and their compositions are consistent with the Phanerozoic counterparts (Fig. 5). Relatively lower Nb concentrations of the studied arc basalts in the range of 2.2 and 2.6 ppm clearly distinguish them from the NEB. The geochemical similarities and variations of the studied samples are evident on the binary relationships of different major, trace and rare earth elements with respect to MgO and Nb in which the boninites form as a different group and NEB exhibit a gradual linear trend with other rock types (Fig. 6).

Chondrite normalized rare earth element (REE) patterns of the boninites display pronounced enrichment in their LREE with moderate to high LREE/MREE fractionation $(La/Sm)_N$ = 2.5–3.4), almost flat HREE patterns with feeble fractionation of MREE/HREE (Gd/Yb_N = 1.18–1.36) and negative Eu anomalies (Eu/Eu^* = 0.76–0.84; Table S2; Fig. 7). They exhibit negative Nb and Ti anomalies on their primitive mantle normalized trace element abundance patterns (Fig. 7). The chondrite normalized REE patterns of the arc basalts are marked by feeble LREE enrichment, slight LREE/HREE fractionations with $(La/Yb)_N$ = 1.86–2.26 and flat HREE patterns. The studied samples display negative Nb and Hf anomalies on their primitive normalized trace element patterns (Fig. 7). The chondrite normalized REE profile for Nb-enriched basalts depicts LREE enriched patterns with prominent LREE/MREE fractionation trends (La/Sm_N = 2.7–3.5). The studied NEBs display negative Nb (Nb/Nb^* = 0.3–0.6) and Ti anomalies compared with their adjacent REE on primitive mantle normalized multi-element patterns (Fig. 7), with Zr/Hf = 43–51; Nb/Ta = 4.0–8.9 and Zr/Sm = 31–41. Chondrite normalized REE patterns for the high magnesian andesites exhibit pronounced LREE enrichment with marked LREE/MREE (La/Sm_N = 2.2–2.7) and LREE/HREE (La/Yb_N = 3.2–4.7)

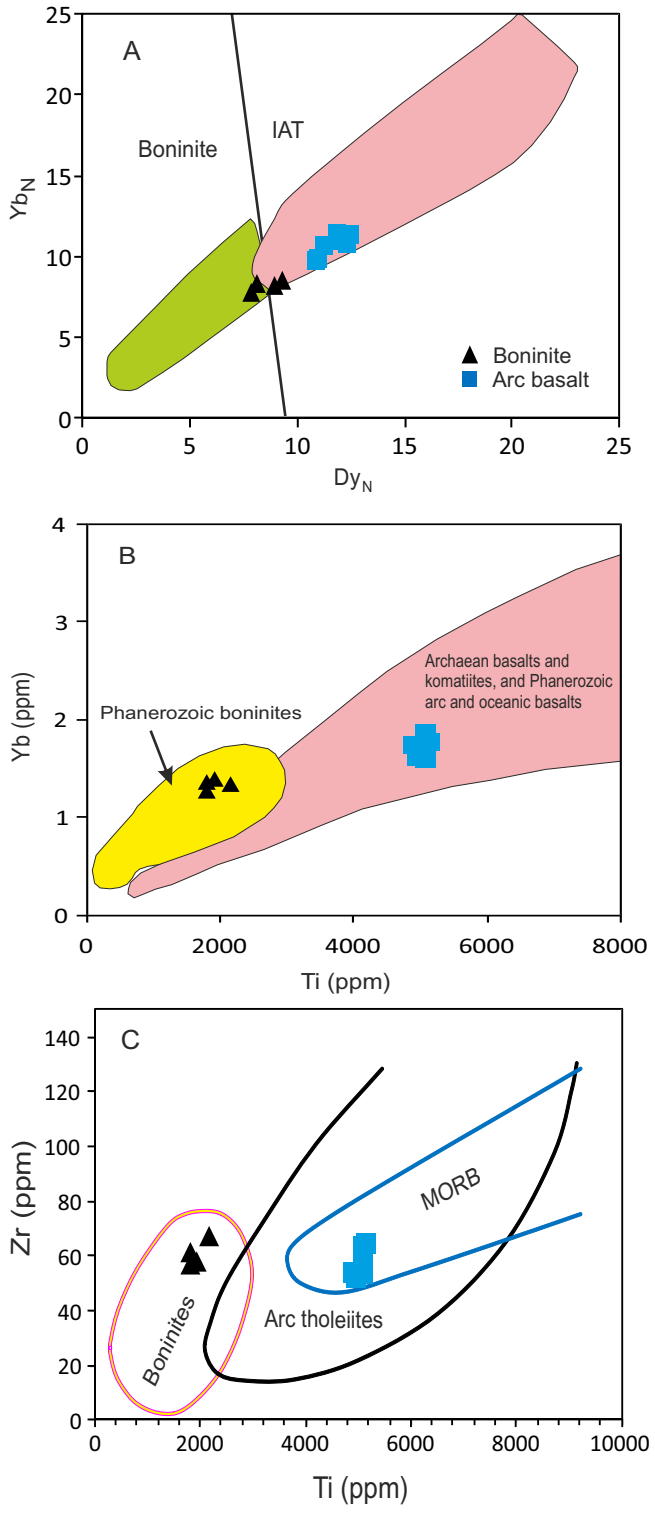

Fig. 4. (A) Dy_N vs. Yb_N discrimination figure showing boninitic and island arc tholeiite characteristics of the studied samples (Saccani, 2015). (B) Ti vs. Yb plot in which the Malangtoli basaltic rocks occupy the field of Phanerozoic boninites and the island arc basalts plot in the field of Archean boninites, komatiites, komatiitc basalts and Phanerozoic arc and oceanic basalts (Poidevin, 1994; Smithies, 2002; Polat et al., 2002). (C) Ti vs. Zr plot in which arc basalts are resembling with MORB composition.

fractionation. All these samples display Th enrichment with respect to the adjacent HFSE on primitive mantle normalized trace element patterns (Fig. 7). The depleted $(Nb/Th)_{pm}$ and $(Nb/La)_{pm}$ ratios, elevated (Th/La)pm, slightly positive Ti anomalies and greater magnitude of negative Nb ($Nb/Nb^* = 0.2–0.3$) anomalies for the high magnesian andesites clearly distinguish them from the NEB (Table S2; Fig. 7). The Zr/Hf, Nb/Ta and Zr/Sm ratios for the boninitic rocks (42–44, 2.3–6.2 and 29–35), arc basalts (50–57, 13–21 and 31–33), high magnesian andesites (40–43, 5.4–17.06 and 34–42)and NEB (43–51, 4.0–8.9 and 31–41) of Malangtoli reflect higher Zr/Hf and Zr/Sm and lower Nb/Ta values compared with the primitive mantle (Zr/Hf = 36, Nb/Ta = 17 and Zr/Sm = 25).

5. Discussion

5.1. Petrogenesis of Malangtoli arc basalts-boninites-HMA-NEB association

The emerging concepts for Archean crustal growth processes have emphasized the role of partial melting of subducted basaltic oceanic crust and infiltration of siliceous melts into the overlying mantle wedge for the origin of adakites, adakitic andesites and HMA that are integral contributors to Archean crust formation (Hollings and Kerrich, 2000; Polat and Kerrich, 2001). Based on Nb/Ta, Zr/Hf and Zr/Sm ratios, Konig and Schuth (2011) and Xiong et al. (2011) have identified different mantle sources that are responsible for the generation of Cenozoic island arc lavas (1) depleted MORB source in the sub-arc mantle wedge, (2) MORB like source with signatures of slab melts having rutile-eclogite residues of cold, deep slabs and (3) melts from hot shallow slabs having amphibole-garnet residue. The Zr/Hf, Nb/Ta and Zr/Sm ratios for the arc basalts, boninitic rocks, HMA and NEB of Malangtoli volcanic suite show higher Zr/Hf and Zr/Sm and lower Nb/Ta values compared with the primitive mantle (Zr/Hf = 36, Nb/Ta = 17 and Zr/Sm = 25) endorsing subduction driven metasomatism, variable contributions from subduction components and enrichment of depleted MORB like mantle source in the sub-arc mantle wedge (Sun and Mc Donough, 1989; Konig and Schuth, 2011; Kerrich and Manikyamba, 2012). The subduction signatures in the studied rock types are corroborated by enrichment in LILE and relative depletion in HFSE. Nd-Hf compositions of arc magmas reveal that in comparison with Hf, Nd behaves as a mobile element in slab-derived fluids/melts. It has been suggested that subduction-metasomatized mantle wedge have increased concentrations of Nd compared to Hf. The LREE-HFSE systematics of the Malangtoli volcanic rocks are marked by elevated abundances of Nd with Hf depletion resulting into high Nd/Hf ratios. These geochemical parameters indicate that metasomatic overprints of wedge melts were controlled by addition of slab derived fluids and melts.

5.1.1. Arc basalts-boninites: juvenile subduction

The tholeiitic to calc-alkaline compositions of arc basalts are equated with a transition from depleted MORB-like to enriched mantle wedge peridotite metasomatized by flux of slab dehydrated fluids rich in incompatible trace elements. Major, trace and rare earth element compositions of boninitic rocks are characterized by high Mg#, MgO, Ni and Cr contents, high Al_2O_3/TiO_2, Zr/Hf ratios with low TiO_2, Zr contents and $(Gd/Yb)_N < 1$ ratios. These geochemical features in conjunction with distinct negative Nb, Ta, Zr, Hf and Ti anomalies on primitive mantle normalized multi-element diagram (Fig. 7), depletion in MREE compared to LREE and HREE, and high La/Sm and low $(Gd/Yb)_N$ ratios collectively attest to magma generation through slab-dehydration and fluid-fluxed metasomatism of mantle wedge in an intraoceanic subduction zone setting. Chondrite normalized REE patterns of the boninitic rocks of Malangtoli lavas are coupled with their $(La/Sm)_N > 1$ and $(Gd/Yb)_N < 1$ features endorsing a refractory mantle source. The LILE and LREE replenishment of the refractory mantle wedge is

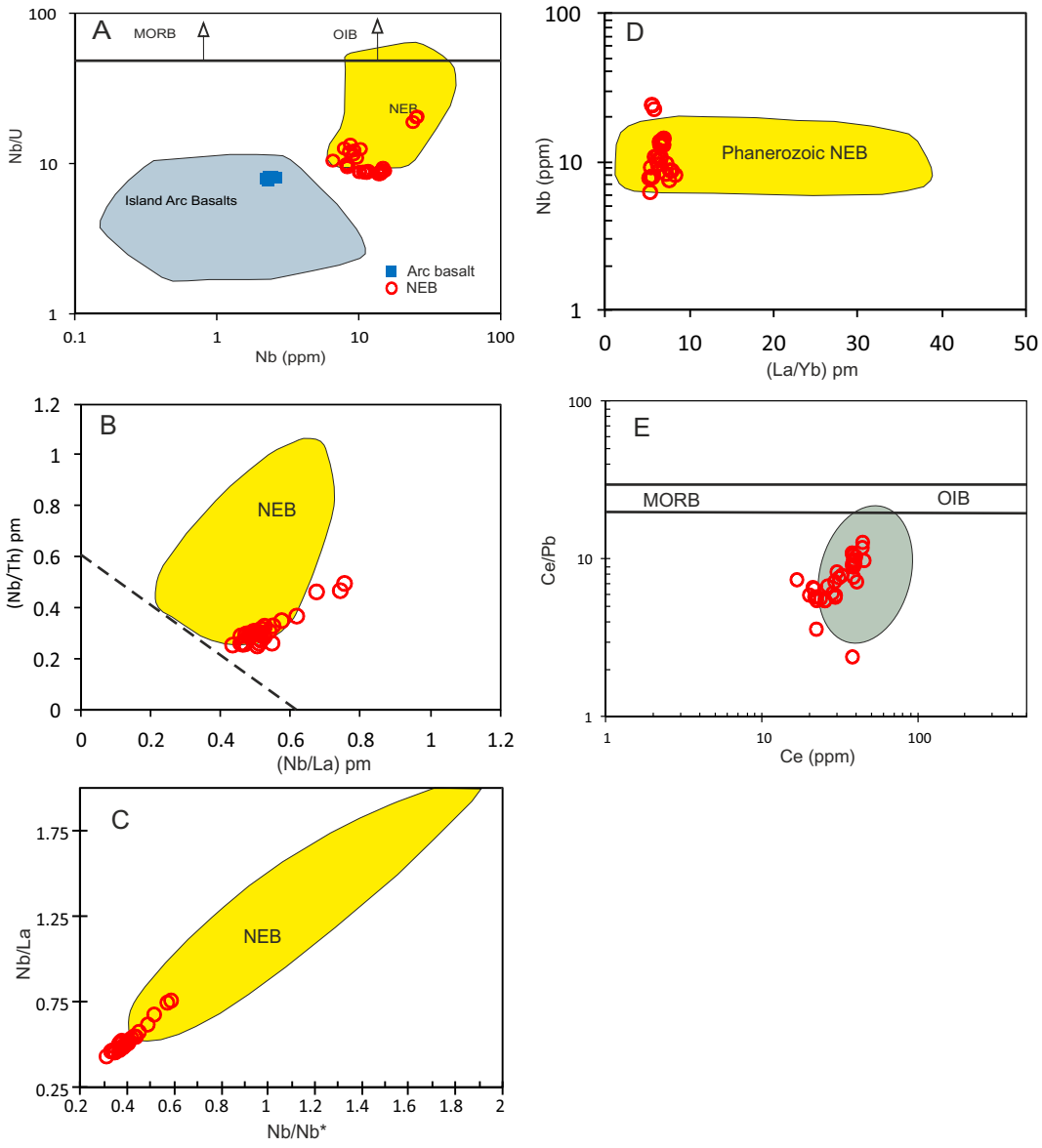

Fig. 5. (A) Nb/U vs. Nb relationship (after Kepezhinskas et al., 1996) showing low and high Nb contents of arc basalts and Nb-enriched basalts (NEB) and their resemblance with the Phanerozoic counterparts; (B) $(Nb/La)_{pm}$ vs. $(Nb/Th)_{pm}$ in which NEB are plotting in the field of Phanerozoic NEB (Sajona et al., 1996; Kepezhinskas et al., 1997; Aguillón-Robles et al., 2001). Dashed line demarcates high ratios of NEB field from the arc basalts and andesites (after Polat and Kerrich, 2001); (C) Nb/Nb^* vs Nb/La relationship in which NEB are occupying the field of Phanerozoic NEB (after Petrone et al., 2006); (D) La/Yb_{pm} vs. Nb of Malangtoli NEB displaying geochemical similarities with Phanerozoic equivalents (fields for Phanerozoic rocks are from Defant et al. (1992), Stern and Kilian (1996), Sajona et al. (1996) and McCarren and Smellie (1998); and (E) Ce vs. Ce/Pb relationship of Malangtoli NEB and their resemblances with Paleozoic NEB from Xinjiang belt, NW China (after Zhang et al., 2005).

attributed to influx of hydrous fluids that are enriched in fluid mobile LILE and LREE, which lowered the solidus temperature and triggered partial melting at shallow level under hydrous conditions. Geochemical studies on Phanerozoic subduction zones suggest a direct relationship between the subduction component and LILE/HFSE ratios. The relative abundance of LILE, HFSE, LREE and their ratios depend on the depth where subducting slab reaches in a subduction zone environment and also on variable interactions between the mantle wedge and subducted slab through dehydration and melting (Hawkesworth et al., 1993). The arc basalts and boninites of Malangtoli represent initial stages of intraoceanic subduction and the petrogenetic processes invoked for the genesis of these rocks include: (i) subduction of oceanic slab, (ii) slab-dehydration and release of fluids enriched in fluid mobile elements (LILE) (iii) fluid-fluxed metasomatism of mantle wedge and high degree partial melting of mantle at shallow depth under high fluid pressure all collectively contributing to generation of arc basalts and boninitic rocks.

5.1.2. High magnesian andesites: slab dehydration or slab melting?

The HMA from Paleoproterozoic Malangtoli volcanic suite exhibit relatively higher concentrations of MgO, Cr and Co compared to normal calc-alkaline andesites of island arc affinity indicating equilibration of parent magma with the peridotitic mantle (Pearce and Peate, 1995; Yogodzinski et al., 1995). These are geochemically analogous to their Phanerozoic counterparts from Setouchi volcanic belt, SW Japan (Tatsumi and Ishizuka, 1982; Tatsumi, 2006), Mt. Shasta, northern California (Grove et al., 2002), Simbo Volcano, Solomon Islands (König et al., 2007), Qiantang terrane, Central Tibet (Wang et al., 2008), Sanchazi block of the Mian Lue ophiolitic melange, central China (Xu et al., 2000) and HMA reported from Archean greenstone belts including Musoma-Mara

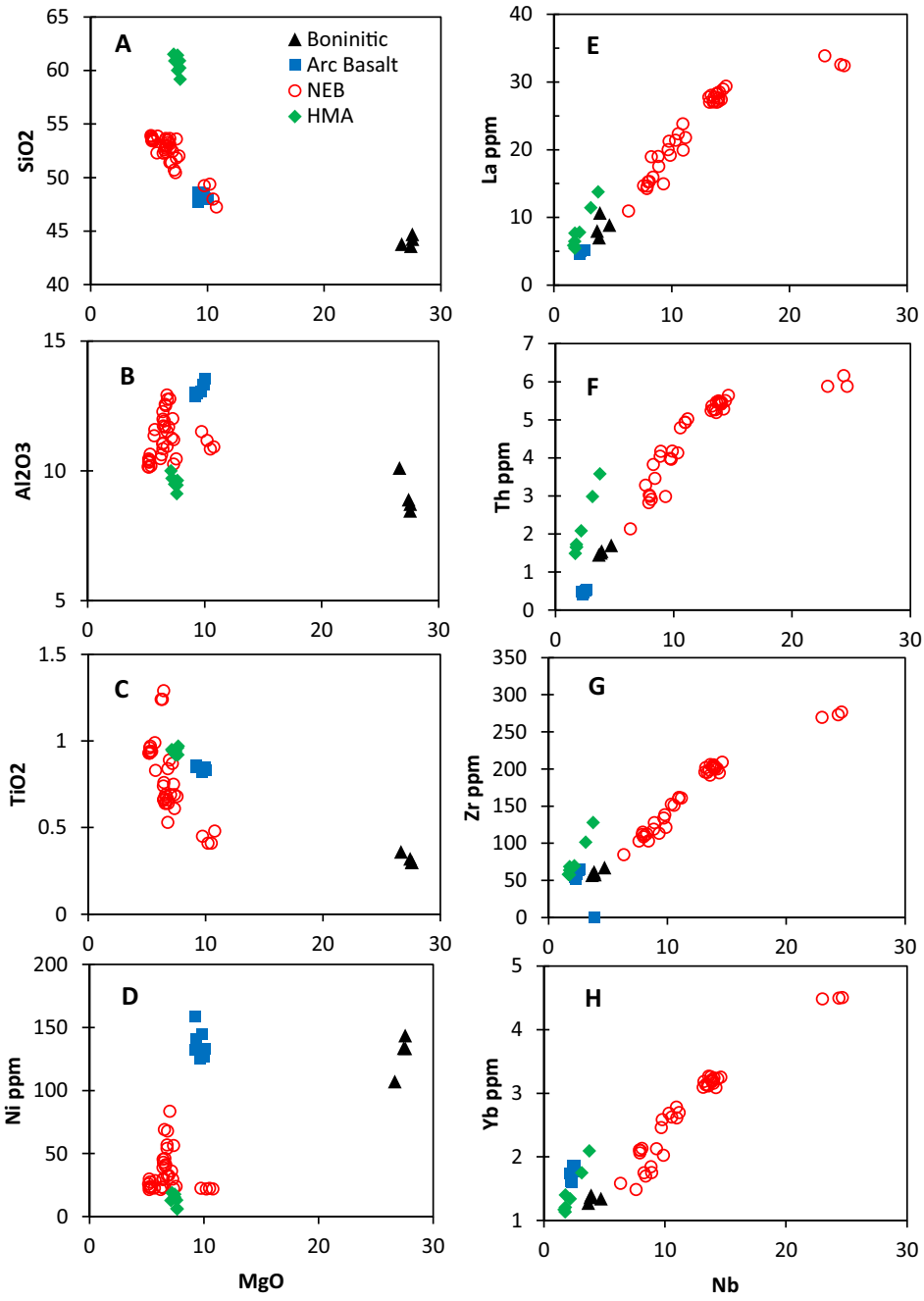

Fig. 6. (A–D) MgO vs. different major elements and Ni and (E–H) Nb vs. highly incompatible (La, Th and Zr) and moderately incompatible element (Yb) exhibiting coherent behaviour of NEB.

greenstone belt, northern Tanzania (Manya et al., 2007), high Mg diorites and magnesian andesites from Wawa greenstone belt of Superior Province, Canada and Pilbara Craton, Australia (Shirey and Hanson, 1984; Smithies and Champion, 2000; Polat and Kerrich, 2001; Manya et al., 2007). However, the petrogenetic processes involved in the origin of these magnesian and high magnesian andesites may not be identical for all cases. The genesis of magnesian and high-magnesian andesites from Simbo Volcano, Solomon Islands; Qiantang terrane, Central Tibet; Sanchazi block of the Mian Lue ophiolitic melange, central China; Wawa greenstone belt of Superior Province, Canada invoke partial melting of mantle wedge that has been hybridized by adakitic melts from subducted slab. Mantle-melt interactions at various intensities and at different stages give rise to high-Mg andesites. High-Mg adakites of Adak and Piip type suggested to have been generated due to variably metasomatized mantle wedge at different stages (Zhang et al., 2005). The high La/Yb (>9), pronounced HREE and Y depletion in magnesian and high magnesian andesites have been ascribed to residual garnet in the source formed by breakdown of pargasitic amphibole during melting of metasomatized mantle wedge (Rogers and Saunders, 1989; Polat and Munker, 2004). Cenozoic magnesian andesites from Mexico, Chile and the Aleutian Islands are suggested to be derived through ridge subduction and adakitic metasomatism of sub arc mantle wedge (Benoit et al., 2002; Polat and Munker, 2004). The genesis of magnesian andesites from Mt. Shasta region of northern California is attributed to a dominance of slab-derived fluids and excludes any contribution from slab melts (Grove et al., 2002). Geochemical interaction

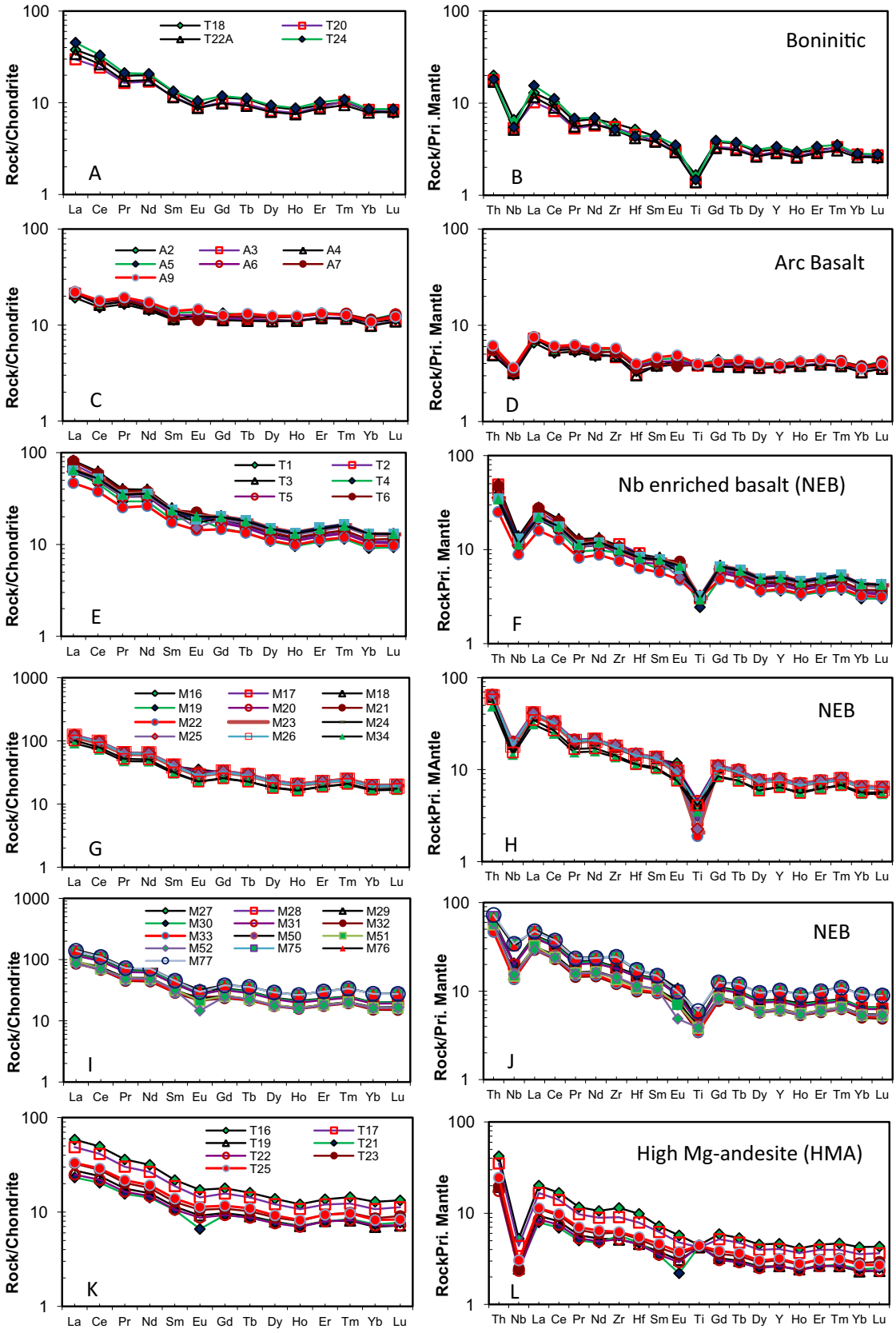

Fig. 7. Chondrite normalized rare earth element (REE) patterns and primitive mantle normalized trace element variation figures of Malangtoli boninitic volcanic rocks, arc basalts, NEB and high Mg-andesites. Normalizing values are from Sun and McDonough (1989).

between asthenospheric melts carrying OIB signature and sub arc mantle wedge metasomatized by slab melts is suggested to be responsible for the generation of magnesian andesites from arc-back arc regimes of Okinawa-Ryukyu and Baja California (Shinjo, 1999; Wang et al., 2002; Calmus et al., 2003). In this case, the melting of subducted oceanic slab was induced by asthenospheric upwelling in a diverging back arc system. Therefore, partial melting of subducted oceanic crust, release of siliceous adakitic melts from subducted slab, hybridization of mantle wedge peridotite by ascending slab melts and partial melting of hybridized mantle wedge are collectively considered responsible for the origin of high magnesian andesites associated with adakitic andesites in hot and young subduction zones (Tatsumi and Ishizuka, 1982; Kelemen, 1990, 1995; Xu et al., 2000; Polat and Munker, 2004). However, in this study, the Malangtoli HMAs are not associated with adakites and plot away from the field of adakites in Sr/Y vs. Y diagrams (Figs. 3B and 8A), showing an affinity towards HMA from Bonin islands. Melts from subducted oceanic slab are characterized by HREE depletion and high La/Yb and Sr/Y due to residual garnet/hornblende in the source. Thus HREE depletion in magmas derived through interaction between subducted eclogitic oceanic crust and mantle wedge is ascribed to residual garnet/amphibole during partial melting. The Malangtoli HMA display moderate LREE enrichment and HREE depletion with lower La/Yb and Sr/Y ratios (Table S2) compared to adakites (19, >40; Wang et al., 2008). These geochemical observations collectively point towards contributions from slab derived fluids that induced metasomatism and partial melting of mantle wedge under hydrous conditions to generate Malangtoli HMA. REE and HFSE signatures of Malangtoli HMA (La/Yb_N = 3.2–4.7; Gd/Yb_N = 1.2–1.3) are not conformable with residual garnet, indicate mantle wedge melting at shallow depth and thus do not support the involvement of slab melts. It is thus envisaged that slab-dehydrated fluids and sediments served as suitable agents for metasomatizing the mantle wedge as potential source for generating Malangtoli HMA at low pressures and high water contents. The La/Yb and Sr/Y ratios for HMA from Setouchi volcanic belt suggest that they are not in equilibrium with residual garnet and the andesitic melts have been produced at relatively low temperatures (1050–1100 °C). Further, it has been advocated that interaction between siliceous melts derived through melting of oceanic slab sediments and mantle wedge peridotite account for the geochemical signatures of Setouchi HMA (Shimoda et al., 1998; Katz et al., 2004). The difference between Malangtoli HMA and those influenced by adakitic metasomatism with residual garnet is that the silicic component for Malangtoli HMA is inherited through dehydration and melting of subducted sediments and not the subducted eclogitic oceanic crust. This contention is also supported by trace and REE compositions for the studied HMA (Fig. 8B). The Th/Yb ratios (1.2–1.7) for the HMA samples are higher than intraoceanic arc lavas (0.05–1.0) and are consistent with the active continental margin magmas (1.0–10.0). This geochemical signature reflects either crustal recycling through sediment influx at subduction zone or minor input from the continental lithosphere and proximity of the Malagntoli HMA with active continental margin.

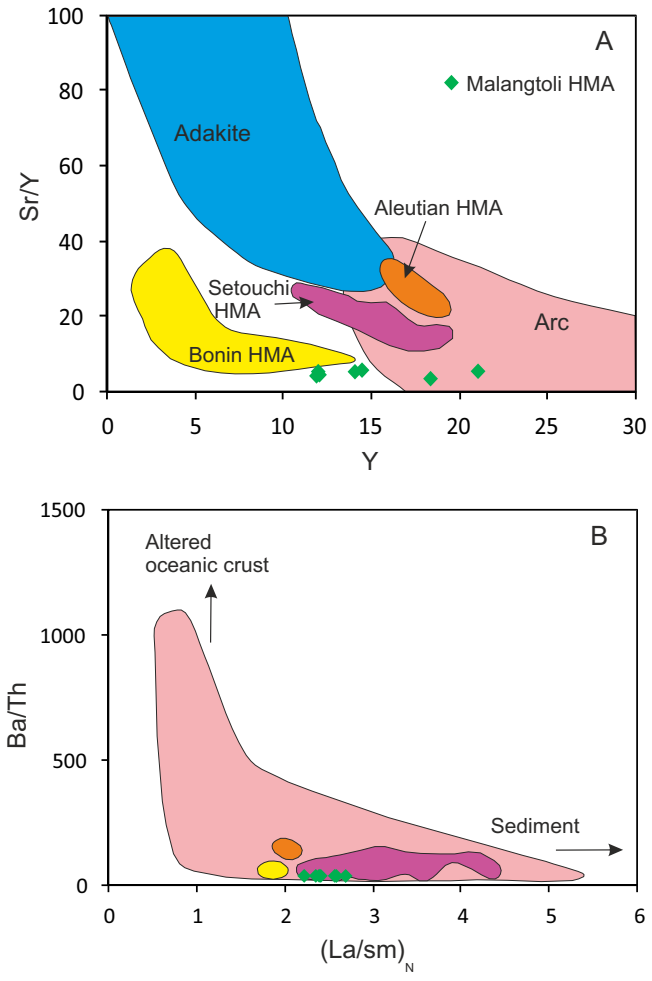

Fig. 8. (A) Y vs. Sr/Y discrimination figure with fields of arc, adakites and high Mg-andesites from Aleutian, Setouchi and Bonin islands in which Malangtoli HMA are falling near the Bonin HMA (after Tatsumi, 2006); (B) Malangtoli HMA resembling with Setouchi HMA on $(La/Sm)_N$ vs. Ba/Th relationship reflecting on sediment contribution to the magma.

5.1.3. Origin of Malangtoli NEB: Arc maturation

Several models that have been proposed to explain the geochemical characteristics of Nb-enriched basalts are (i) Partial melting of the subducted oceanic crust, (ii) partial melting of enriched mantle carrying an OIB component (iii) crustal/sediment assimilation by the ascending magma and (iv) melting of hybridized mantle wedge above a subduction zone (Zhang et al., 2005; Wang et al., 2007). Experimental studies have demonstrated that partial melting of a subducted oceanic slab produces siliceous melts of adakitic compositions (Defant et al., 1992; Hastie et al., 2011) and cannot account for the formation of magmas with higher Nb content and associated geochemical characteristics typical of NEBs (Rapp et al., 1999; Zhang et al., 2005). The lower Nb/U and Ce/Pb ratios of Malangtoli NEB do not support their generation by melting of OIB/enriched mantle source (Fig. 5A and E). Magmas derived from OIB source are characterized by positive Nb anomalies. However, the studied Malangtoli samples with marked Nb enrichment show negative Nb anomalies which discard the possibility of OIB component in the mantle source. The Nb enrichment with lower LILE/HFSE ratios of the studied NEB rules out crustal/sediment assimilation during magma ascent which otherwise would have resulted into extremely elevated LILE concentrations. Though NEBs are very rare and identified from only few cratons till date (Hollings and Kerrich, 2000; Polat and Kerrich, 2001; Manikyamba and Khanna, 2007; Petrone and Ferrari, 2008; Wang et al., 2008; Kerrich and Manikyamba, 2012), the available data suggest that these are characteristic rock type generated at convergent margin processes where slab melts play a vital role in the metasomatism of the mantle wedge. The usual occurrence of adakites with NEB strongly supports their genetic link during the convergent margin processes. The HFSE enrichment in these rocks have been equated with (i) melting of young (⩽20–30 Ma), hot, subducted oceanic lithosphere under garnet amphibolite to eclogite facies conditions (ii) metasomatism and hybridization of mantle wedge by slab melts

(iii) presence of asthenospheric or lithospheric OIB component in the mantle wedge and (iv) incorporation of subducted sediments or assimilation of continental materials during magma ascent (Wyman et al., 2000; Zhang et al., 2005; Wang et al., 2007, 2008).

Kepezhinskas et al. (1996) identified preferential enrichment of HFSE in the Na-metasomatized mantle which subsequently melted and gave rise to Nb-enriched basalts (Zhang et al., 2005). Rapp et al. (1999) experimentally demonstrated the reaction between amphibole melt (adakitic) and spinel lherzolite to give rise Na-amphibole and orthopyroxene. According to Ayers (1998), the Nb-Ta partition coefficients are very high for rutile and its melts, the mantle peridotite can scavenge them during slab melt-wedge interaction which will be hosted in pyroxene, olivine, garnet and spinel. However, the experimental studies suggest that the D-value of Nb between amphibole and slab melts is low (0.02–0.20; Green, 1994). Amphibole is the most common Nb-bearing metasomatized phase in NEB (Ionov and Hofmann, 1995; Sajona et al., 1993, 1996). However, amphibole-ilmenite or amphibole-orthopyroxene also host Nb-Ta during the generation of NEB (Hollings and Kerrich, 2000; Polat and Kerrich, 2001). As amphibole is the most common mineral phase during the slab-wedge interaction, it is the common host for Nb in the melting of metasomatized mantle peridotite (Zhang et al., 2005). The geochemical signatures of the Malangtoli NEB support their generation through the melting of mantle wedge metasomatized by slab melts (Kepezhinskas et al., 1996; Defant et al., 1992; Defant and Drummond, 1993; Sajona et al., 1993, 1996; Zhang et al., 2005) which is also evidenced from NEBs reported from the greenstone belts of Dharwar Craton (Manikyamba and Khanna, 2007; Kerrich and Manikyamba, 2012), Canada (Hollings and Kerrich, 2000; Wyman et al., 2000; Polat and Kerrich, 2001; Hollings, 2002) and other Phanerozoic volcanic sequences (Wang et al., 2008; Hastie et al., 2011).

Sajona et al. (1993, 1996) and Kepezhinskas et al. (1995, 1996) suggested that melts of subducted oceanic slab are produced at >700 °C and 75–85 km depth. These slab melts carry greater amount of LREE and HFSE than the hydrous fluids and they ascend to percolate through the mantle wedge resulting into its hybridization and metasomatism. The reaction between slab melts and mantle wedge peridotite breaks down olivine, orthopyroxene, clinopyroxene and spinel forming Nb and Ti enriched pargasitic amphibole, garnet, phlogopite, Na-rich clinopyroxene and Fe-rich orthopyroxene. Trace and rare earth element systematics of Malangtoli HMA indicate partial melting of a peridotitic mantle hybridized by adakitic melt-mantle wedge interaction while a mantle residue carrying Nb enriched phases (amphibole, ilmenite) is left behind. These metasomatic minerals trap HFSE (Nb, Ti, Ta) and decomposition of these phases in the convecting mantle peridotite trigger partial melting at depths above the zone of slab melting generating NEB. Therefore, the origin of Malangtoli NEB is interpreted in terms of (i) migration of slab melts carrying fluid immobile HFSE and LREE elements to the sub arc mantle wedge (ii) metasomatism, hybridization and HFSE enrichment of mantle wedge peridotite by percolating slab melts (iii) decomposition of Nb-bearing phases (amphibole, ilmenite) inducing partial melting and derivation of NEB.

5.2. Geodynamic implications: Subduction initiation to arc maturation

The identification of boninites, NEB, Mg-andesites and adakites from Phanerozoic subduction zones led many workers to revisit the Archean and Proterozoic volcano-sedimentary sequences and recorded such associations from different parts of the world (Polat and Kerrich, 2006 and references therein; Zhang et al., 2005; Manikyamba et al., 2005; Manikyamba and Khanna, 2007; Petrone and Ferrari, 2008; Castillo, 2009; Kerrich and Manikyamba, 2012; Mao et al., 2012; Aguillón-Robles et al., 2001). The geochemical systematics of NEB and associated lithologies from Archean terranes testify the operation of Phanerozoic type subduction processes during Precambrian time. The resemblance of Malangtoli NEB with Phanerozoic NEBs is evidenced by the behaviour of their LREE/HREE with Nb and Ce vs. Ce/Pb ratios where the Malangtoli samples are occupying the fields of Phanerozoic NEB and field of Paleozoic NEB from Xinjiang, northwest China (Zhang et al., 2005; Fig. 5). Malangtoli NEB are geochemically analogous to the NEB reported from the Neoarchean Penakacherla greenstone belt of Dharwar Craton, India and other Cenozoic NEB in oceanic arcs (Polat and Kerrich, 2006; Kerrich and Manikyamba, 2012; Wang et al., 2008). The Malangtoli NEBs of Singhbhum Craton exhibit negative Nb anomalies (Singh et al., 2016) in common with NEB from Penakacherla and other Archean cratons whereas the NEB from Neoarchean Gadwal greenstone belt of Dharwar Craton, India, exhibit pronounced positive Nb anomalies The trace element signatures of NEB from the Neoarchean Penakacherla greenstone belt (Dharwar Craton, India; Kerrich and Manikyamba, 2012), Wawa greenstone belt (Superior Province, Canada) and Cenozoic counterparts (Panama, Northern Kamchatka, Philippines, Baja California (Defant et al., 1992; Kepezhinskas et al., 1996; Sajona et al., 1996; Benoit et al., 2002; Polat and Kerrich, 2006) collectively indicate consistent geochemical behaviour with the Malangtoli NEB. Mildly fractionated REE of the studied NEBs reflect the derivation of melt components from deeper source with residual garnet which is similar with the Phanerozoic and Archean counterparts (Hirschmann and Stolper, 1996; Kerrich and Manikyamba, 2012).

The Singhbhum Craton of eastern India has excellent preservation of volcano-sedimentary sequences representing the time span of Paleo-Mesoarchean to Proterozoic representing various geodynamic scenarios. Though a large volume of geochronological data is available on various formations of Singhbhum Craton, characterization of these lithounits in terms of their LILE, HFSE, REE and platinum Group elements (PGE), demarcating their geodynamic setting is very limited. Based on the identification of a wide spectrum of volcanic rocks from the Phanerozoic subduction zones, the greenstone belts of various cratons around the globe have been revisited and similar lithological associations with comparable geochemical characteristics have been recognized from many greenstone belts of India, Canada, China, Australia, Zimbabwe and Greenland. This observation endorses the existence of Phanerozoic type of plate tectonic processes during Archean and Proterozoic. However, keeping in view the higher geothermal gradient during Archean, the Archean plate tectonic processes might have operated at a different scale. According to Sajona et al. (1996) the generation of NEBs involves the reaction of slab derived melts with the sub-arc mantle peridotite during the shallow subduction of young and hot oceanic lithosphere. When the melts erupt directly to the surface, they form adakites. However, if the mantle wedge peridotite is metasomatically altered and hybridized by the adakitic slab melts, then partial melting of the hybridized peridotite will produce HMA. In this process HFSE has been scavenged by amphibole and Fe-rich orthopyroxenes and a HFSE-enriched hybridized residue is formed ensuing the eruption of HMA. Subsequently, subduction-driven convection drags the sub-arc mantle to depths where it melts and generates NEB (Sajona et al., 1996; Hollings and Kerrich, 2000). The geochemical features of NEB are best explained through adakite-HMA-NEB association. However, in the absence of adakite data, the available geochemical parameters support genesis of Malangtoli HMA through mantle wedge metasomatism by slab-dehydrated fluids and sediments and that of NEB through mantle wedge hybridization by HFSE enriched slab melt. The crustal signatures in these HMA and NEB may reflect their origin between arc-back arc regions. The genesis

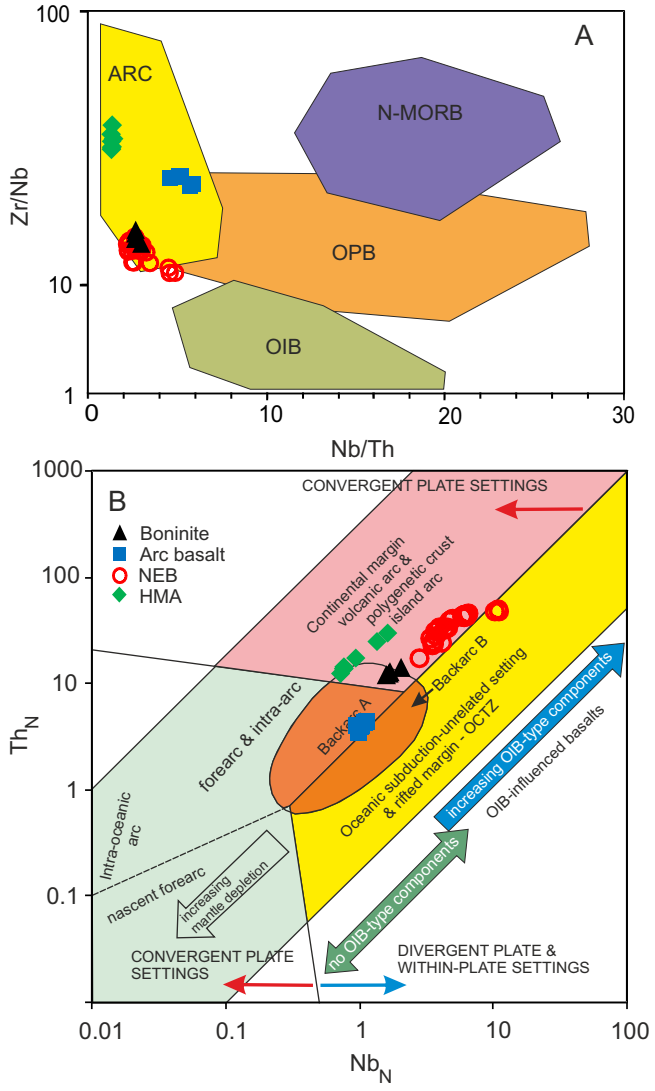

Fig. 9. (A) Nb/Th vs. Zr/Nb (after Zhao and Zhou, 2007) displaying arc characteristics of Malangtoli volcanic suite and (B) Nb_N vs. Th_N tectonic discrimination figure (after Saccani, 2015) in which arc basalts indicate back arc setting whereas boninites, NEB and HMA display continental margin volcanic arc with polygenetic crustal signatures.

of Malangtoli NEB is thus associated with mantle wedge metasomatism by melts of subducted oceanic slab and these are generated at transitional arc to rift-controlled back arc tectonic regime in a basinal environment that developed proximal to an active convergent margin setting. Zr/Nb vs. Nb/Th tectonic discrimination plot (Fig. 9A) suggest subduction-related arc setting for the studied volcanic rocks. In Th_N vs. Nb_N diagram (Fig. 9B), the arc basalts correspond to a back arc setting, while the boninite, HMA and NEB samples occupy the field of continental margin volcanic arc and island arc with polygenetic crustal signatures.

It is thus envisaged that arc basalt-boninite-HMA-NEB association from Malangtoli preserves the signature of a spectrum of Paleoproterozoic convergent margin magmatic processes in Singhbhum Craton spanning from subduction initiation to arc maturation (Fig. 10). The presence of HMA and NEB in the Malangtoli lavas gives future directions to explore the adakites in this part of Singhbhum Craton. The important petro-tectonic processes invoked for the genesis of these rocks include: (i) subduction of oceanic slab, (ii) slab-dehydration and release of fluids enriched in fluid immobile elements (LILE), (iii) fluid-fluxed metasomatism of mantle wedge and high degree partial melting of mantle at shallow depth under high fluid pressure collectively contributing to generation of arc basalts and boninitic rocks, (iv) hydrous melting of mantle wedge peridotite metasomatized by slab dehydrated fluids and sediments account for the generation of HMA, (v) melting of the subducted slab, interaction between sub-arc mantle peridotite and siliceous slab melts forming HFSE enriched phases and (vi) decomposition of Nb-bearing phases in convecting mantle at depths promoting low degree partial melting of the HFSE-enriched, hybridized peridotite with garnet as residual phase giving rise to NEB. Arc basalts and boninites are interpreted to be the products of initial stages of intraoceanic subduction, while derivation of HMA and NEB reflect slab-melting and mantle wedge hybridization processes corroborating intermediate to matured stages of subduction (Fig. 10).

6. Conclusions

- The arc basalt-boninite-HMA-NEB association from 2.25 Ga Malangtoli volcanic suite of Singhbhum Craton with distinct geochemical signature reflect various stages of subduction and variable contributions from subduction-derived metasomatizing agents.

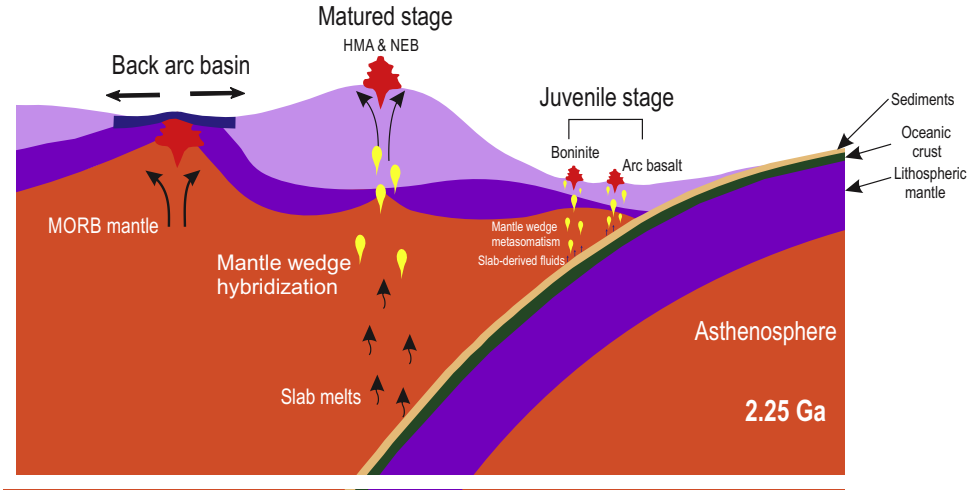

Fig. 10. Schematic tectonic model explaining the genesis of Paleoproterozoic Malangtoli volcanic suite of Singhbhum Craton in which boninitic volcanic rocks along with arc basalts erupted during the initial stage whereas the NEB and HMA were generated at the matured stage of subduction zone processes.

- The mafic volcanic rocks having low SiO_2 (<45 wt.%), high Mg# (0.8) MgO (>25 wt.%), Ni and Cr contents, high Al_2O_3/TiO_2 (>20), Zr/Hf ratios with low TiO_2, Zr concentrations, $(La/Sm)_N > 1$ and $(Gd/Yb)_N < 1$ ratios attesting to their boninitic characters.
- The high SiO_2 (>54 wt.%), MgO (>6 wt.%), Mg# with elevated Cr, Co, Ni and Th contents, depleted $(Nb/Th)_N$, $(Nb/La)_N$, high $(Th/La)_N$ ratios, moderate depletion in HREE and Y with La/Yb < 9 and low Sr/Yclassify them as HMA.
- The calc-alkaline basalts with higher Nb contents (6.3–24 ppm), lower magnitude of negative Nb anomalies, high $(Nb/Th)_{pm}$ = 0.28–0.59, $(Nb/La)_{pm}$ = 0.40–0.69 and Nb/U = 2.8–34.4 compared to normal arc basalts [Nb = <2 ppm; $(Nb/Th)_{pm}$ = 0.10–1.19; $(Nb/La)_{pm}$ 0.17–0.99 and Nb/U = 2.2–44 respectively] differentiate them as NEB.
- The Malangtoli HMA and NEB are geochemically analogous to their Archean and Phanerozoic counterparts.
- Arc basalts and boninites are interpreted to be the products of shallow level partial melting of mantle wedge under hydrous conditions during juvenile stages of intraoceanic subduction. The geochemical signatures of HMA are conformable with partial melting of mantle wedge metasomatized by slab-dehydrated fluids and sediments under hydrous conditions during the intermediate stage of subduction.
- Extraction of arc basalts, boninitic and HMA melts and slab melting at matured stages of subduction rendered the mantle wedge hybridized and enriched in HFSE which on low degree partial melting with residual garnet generated the NEB.
- The crustal signatures in HMA and NEB are attributed to recycling of older continental crust or their genesis in between the arc-back arc region proximal to active continental margin environment.

Acknowledgements

The authors are grateful to Dr. V.M. Tiwari, Director, CSIR-NGRI for permitting to publish this work. We thank two anonymous reviewers for their constructive reviews and Prof. Manoj Pandit for editorial handling. We acknowledge the funds received from Department of Science and Technology, India (SR/S4/ES-510/2010) and India Deep Earth Exploration Programme (INDEX) for conducting these studies. M.R.S acknowledges the CSIR – India SRF funds (No. 131097/2K14/1-EMR1). This study also contributes to the Talent Award to Prof. M. Santosh under the 1000 Plan from the Chinese Government. We thank the help of Ms. Adrija Chatterjee and Ms. P. Madhuparna during the field work and Drs. A. K. Krishna, M. Satyanarayanan, K.S.V. Subramanyam and S.S. Sawant in generating the geochemical data.

Appendix A. Supplementary material

Supplementary data associated with this article can be found, in the online version, at http://dx.doi.org/10.1016/j.jseaes.2016.09.015.

References

Aguillón-Robles, A., Calmus, T., Benoit, M., Bellon, H., Maury, R., Cotton, J., Bourgois, J., Michard, F., 2001. Late Miocene adakites and Nb-enriched basalts from Vizcaino Peninsula, Mexico: indicators of East Pacific Rise subduction below southern Baja California. Geology 29, 531–534.

Ayers, J., 1998. Trace element modeling of aqueous fluid-peridotite interaction in the mantle wedge of a subduction zone. Contrib. Miner. Petrol. 132, 390–404.

Banerjee, M., Ray, J., Nandy, S., Manikyamba, C., Madhuparna, P., Chakraborthy, D., Eslami, A., 2016. Experimental studies to constrain parental magma of Malangtoli volcanics from Singhbhum craton of eastern Indian shield. J. Geol. Soc. India 88, 245–255.

Benoit, M., Aguillón-Robles, A., Calmus, T., Maury, R., Bellon, H., Cotton, J., Bourgois, J., Michard, F., 2002. Geochemical diversity of Late Miocene volcanism in southern Baja California, Mexico: implication of mantle and crustal sources during the opening of an asthenospheric window. J. Geol. 110, 627–648.

Bose, M.K., 2000. Mafic-ultramafic magmatism in the eastern Indian craton – a review. Geology Survey of India. Special Publication No. 55, pp. 227–258.

Bose, M.K., 2009. Precambrian mafic magmatism in the Singhbhum Craton, eastern India. J. Geol. Soc. India 73, 13–35.

Calmus, T., Aguillon-Robels, A., Maury, R.C., Bellon, H., Benoit, M., Cotton, J., Bourgois, J., Michaud, F., 2003. Spatial and temporal evolution of basalts and magnesian andesites (“bajaites”) from Baja California, México: the role of slab melts. Lithos 66, 77–105.

Castillo, P.R., 2009. Origin of Nb-enriched basalts and adakites in Baja California, Mexico, revised: Reply. GSA Bull. 121, 1470–1472.

Defant, M.J., Drummond, M.S., 1990. Derivation of some modem arc magmas by melting of young subduction lithosphere. Nature 347, 662–665.

Defant, M.J., Jackson, T.E., Drummond, M.S., 1992. The geochemistry of young volcanism throughout western Panama and southeastern Costa Rica: An overview. J. Geol. Soc. London 149, 569–579.

Defant, M.J., Drummond, M.S., 1993. Mount St. Helens: potential example of the partial melting of the subducted lithosphere in a volcanic arc. Geology 21, 547–550.

Defant, M.J., Kepezhinskas, P., 2001. Evidence suggests slab melting in arc magmas. EOS Trans., Am. Geophys. Union 82, 67–69.

Elburg, A.M., van-Bergen, V.M., Hoogewerff, J., Foden, J., Vroon, P., Zulkarnain-Iskandar, I., Nasution-Asnawir, A., 2002. Geochemical trends across an arc-continent collision zone; magma sources and slab-wedge transfer processes below the Pantar Strait volcanoes, Indonesia. Geochim. Cosmochim. Acta 66, 2771–2789.

Elliot, T., Plank, T., Zindler, A., White, W., Bourdon, B., 1997. Element transport from slab to volcanic front at the Mariana arc. J. Geophys. Res. 102, 14991–15019.

Eriksson, P.G., Mazumder, R., Catuneanu, O., Bumby, A.J., Ountsche Ilondo, B., 2006. Precambrian continental freeboard and geological evolution: a time perspective. Earth-Sci. Rev. 79, 165–204.

Govindaraju, K., 1994. Compilation of working values and sample description for383 geostandards. Geostandard Newslett. 18, 1–158.

Green, T.H., 1994. Experimental studies of trace element partitioning applicable to igneous petrogenesis: Sedona, 16 years later. Chem. Geol. 117, 1–36.

Grove, T.L., Parman, S.W., Bowring, S.A., Price, R.C., Baker, M.B., 2002. The role of an H_2O-rich fluid component in the generation of primitive basaltic andesites and andesites from the Mt. Shasta region, N California. Contrib. Miner. Petrol. 142, 375–396.

Hastie, A.R., Mitchell, S.F., Kerr, A.C., Minifie, M.J., Millar, I.L., 2011. Geochemistry of rare high-Nb basalt lavas: are they derived from a mantle wedge metasomatised by slab melts? Geochim. Cosmochim. Acta 75, 5049–5072.

Hawkesworth, C.J., Gallagher, K., Hergt, J.M., 1993. Mantle and slab contributions in arc magmas. Annu. Rev. Earth Planet. Sci. 21, 175–204.

Hirschmann, M.M., Stolper, E.M., 1996. A possible role for garnet pyroxenite in the “garnet signature” in MORB. Contrib. Miner. Petrol. 124, 185–208.

Hollings, P., 2002. Archean Nb-enriched basalts in the northern Superior Province. Lithos 64, 1–14.

Hollings, P., Kerrich, R., 2000. An Archean arc basalt-Nb-enriched basalt-adakite association: the 2.7 Ga Confederation assemblage of the Birch-Uchi greenstone belt, Superior Province. Contrib. Miner. Petrol. 139, 208–226.

Ionov, D.A., Hofmann, A.W., 1995. Nb-Ta-rich mantle amphiboles and micas: implications for subduction-related metasomatic trace element fractionations. Earth Planet. Sci. Lett. 131, 341–356.

Iyengar, S.V.P., Murthy, Y.G.K., 1982. The evolution of the Archean-Proterozoic crust in parts of Bihar and Orissa, eastern India. Rec. Geol. Surv. India 112, 1–5.

Iwamori, H., Nakamura, H., 2015. Isotopic heterogeneity of oceanic, arc and continental basalts and its implications for mantle dynamics. Gondwana Res. 27, 1131–1152.

Katz, O., Beyth, M., Miller, N., Stern, R., Avigad, D., Basu, A., Anbar, A., 2004. A Late Neoproterozoic (V630 Ma) high-magnesium andesite suite from southern Israel: implications for the consolidation of Gondwanaland. Earth Planet. Sci. Lett. 218, 475–490.

Kelemen, P.B., 1990. Reaction between ultramafic rock and fractionating basaltic liquid I. Phase relations, the origin of calc-alkaline magma series, and the formation of discordant dunite. J. Petrol. 31, 51–98.

Kelemen, P.B., 1995. Genesis of high Mg-andesites and the continental crust. Contrib. Miner. Petrol. 120, 1–19.

Kepezhinskas, P.K., Defant, M.J., Drummond, M.S., 1995. Na metasomatism in the island-arc mantle by slab melt-peridotite interaction: evidence from mantle xenoliths in the North Kamchatka arc. J. Petrol. 36, 1505–1527.

Kepezhinskas, P.K., Defant, M.J., Drummond, M.S., 1996. Progressive enrichment of island arc mantle by melt–peridotite interaction inferred from Kamchatka xenoliths. Geochim. Cosmochim. Acta 60, 1217–1229.

Kepezhinskas, P.K., McDermott, F., Defant, M.J., Hochstaedter, A., Drummond, M.S., Hawkesworth, C.J., Koloskov, A., Maury, R.C., Bellon, H., 1997. Trace element and Sr-Nd-Pd isotopic constraints on a three component model of Kamchatka arc petrogenesis. Geochim. Cosmochim. Acta 61, 577–600.

Kerrich, R., Manikyamba, C., 2012. Contemporaneous eruption of Nb-enriched basalts – K-adakites – Na-adakites from the 2.7 Ga Penakacherla terrane: implications for subduction zone processes and crustal growth in the eastern Dharwar craton, India. Canadian J. Earth Sci. 49, 615–636.

Kimura, J.-I., Yoshida, T., 2006. Contributions of slab fluid, mantle wedge and crust to the origin of Quaternary Lavasin the NE Japan Arc. J. Petrol. 47, 2185–2232.
Kimura, J.-I., Nakajima, J., 2014. Behaviour of subducted water and its role in magma genesisin the NE Japan arc: a combined geophysical and geochemical approach. Geochim. Cosmochim. Acta 143, 165–188.
Konig, S., Schuth, S., 2011. Deep melting of old subducted oceanic crust recorded by superchondritic Nb/Ta in modern island arc lavas. Earth Planet. Sci. Lett. 301, 265–274.
König, S., Schuth, S., Münker, C., Qopoto, C., 2007. The role of slab melting in the petrogenesis of high Mg andesites: Evidence from Simbo volcano, Solomon Islands. Contrib. Miner. Petrol. 153, 85–103.
Li, Y.-B., Kimura, J.-I., Machida, S., Ishii, T., Ishiwatari, A., Maruyama, S., Qiu, H.-N., Ishikawa, T., Kato, Y., Haraguchi, S., Takahata, N., Hirahara, Y., Miyazaki, T., 2013. High-Mg adakite and low-Ca boninite from a Bonin fore-arc seamount: implications for the reaction between the slab melts and depleted mantle. J. Petrol. 54, 1149–1175.
Liu, Y., Santosh, M., Yuan, T., Li, H., Li, T., 2015. Reduction of buried oxidized oceanic crust during subduction. Gondwana Res. http://dx.doi.org/10.1016/j.gr.2015.02.014.
Manikyamba, C., Khanna, T.C., 2007. Crustal growth processes as illustrated by the Neoarchean intraoceanic magmatism from Gadwal greenstone belt, eastern Dharwar Craton, India. Gondwana Res. 11, 476–491.
Manikyamba, C., Kerrich, R., 2012. Eastern Dharwar Craton, India: continental lithosphere growth by accretion of diverse plume and arc terranes. Geosci. Front. 3, 225–240.
Manikyamba, C., Naqvi, S.M., Rao, D.V.S., Mohan, M.R., Khanna, T.C., Rao, T.G., Reddy, G.L.N., 2005. Boninites from the Neoarchean Gadwal greenstone belt, eastern Dharwar Craton, India: implications for Archean subduction processes. Earth Planet. Sci. Lett. 230, 65–83.
Manikyamba, C., Kerrich, R., Khanna, T.C., Krishna, A.K., Satyanarayanan, M., 2008. Geochemical systematics of komatiite-tholeiite and adakite-arc basalt associations: the role of a mantle plume and convergent margin in formation of the Sandur Superterrane, Dharwar Craton. Lithos 106, 155–172.
Manikyamba, C., Kerrich, R., Khanna, T.C., Satyanarayanan, M., Krishna, A.K., 2009. Enriched and depleted arc basalts, with high-Mg andesites and adakites: a potential paired arc-backarc of the 2.7 Ga Hutti greenstone terrane, India. Geochim. Cosmochim. Acta 73, 1711–1736.
Manikyamba, C., Ray, J., Ganguly, S., Rajanikanta Singh, M., Santosh, M., Saha, A., Satyanarayanan, M., 2015. Boninitic metavolcanic rocks and island arc tholeiites from the Older Metamorphic Group (OMG) of Singhbhum Craton, eastern India: geochemical evidence for Archean subduction processes. Precambr. Res. 271, 138–251.
Manya, S., Maboko, M.A.H., Nakamura, E., 2007. The geochemistry of high-Mg andesite and associated adakitic rocks in the Musom Mara Greenstone Belt, northern Tanzania: possible evidence for Neoarchaean ridge subduction? Precambr. Res. 159, 241–259.
Mao, Q., Xiao, W., Fang, T., Wang, J., Han, C., Sun, M., Yuan, C., 2012. Late Ordovician to early Devonian adakites and Nb-enriched basalts in the Liuyua area, Beishan, NW China: implications for early Paleozoic slab-melting and crustal growth in the southern Altaids. Gondwana Res. 22, 534–553.
Martin, H., 1986. Effect of Steeper Archean geothermal gradient on geochemistry of subduction zone magmas. Geology 14, 753–756.
McCarren, J.J., Smellie, J.L., 1998. Tectonic implications of fore-arc magmatism and generation of high-magnesian andesites: Alexander Island, Antarctica. J. Geol. Soc., London 155, 269–280.
McCulloch, M.T., Gamble, A.J., 1991. Geochemical and geodynamical constraints on subduction zone magmatism. Earth Planet. Sci. Lett. 102, 358–374.
Mazumder, R., 2005. Proterozoic sedimentation and volcanism in the Singhbhum crustal province, India and their implications. Sed. Geol. 176, 167–193.
Mazumder, R., Reddy, S., Clark, C., 2010. Temporal constraints on the evolution of the Singhbhum Crustal Province from U-Pb SHRIMP data. In: Tyler, I.M., Knox-Robinson, C.M. (Eds.), Fifth International Archean Symposium Abstracts. Geological Survey of Western Australia, p. 193. Record 2010/18.
Misra, S., Johnson, P.T., 2005. Geochronological constraints on the evolution of the Singhbhum Mobile Belt and associated basic volcanics of eastern Indian shield. Gondwana Res. 8, 129–142.
Misra, S., 2006. Precambrian chronostratigraphic growth of Singhbhum-Orissa Craton, Eastern Indian Shield: an alternative model. J. Geol. Soc. India 67, 356–378.
Mohanty, S., 2012. Spatio-temporal evolution of the Satpura Mountain Belt of India: a comparison with the Capricorn Orogen of Western Australia and implication for evolution of the supercontinent Columbia. Geosci. Front. 3, 241–267.
Mondal, S.K., 2009. Chromite and PGE deposits of Mesoarchaean ultramafic-mafic suites within the greenstone belts of the Singhbhum Craton, India: implications for mantle heterogeneity and tectonic setting. J. Geol. Soc. India 73, 36–51.
Mukhopadhyay, D., 2001. The Archean nucleus of Singhbhum: the present state of knowledge. Gondwana Res. 4, 307–318.
Mukhopadhyay, J., Ghosh, G., Zimmermann, U., Guha, S., Mukherjee, T., 2012. A 3.51 Ga bimodal volcanics-BIF-ultramafic succession from Singhbhum Craton: implications for Paleoarchean geodynamic processes from the oldest greenstone succession of the Indian sub-continent. Geol. J. 47, 284–311.
Mukhopadhyay, J., Crowley, Q.G., Ghosh, S., Ghosh, G., Chakrabarti, K., Misra, B., Heron, K., Bose, K., 2014. Oxygenation of the Archean atmosphere: new paleosol constraints from eastern India. Geology. http://dx.doi.org/10.1130/G36091.1.
Mullen, E.K., McCullum, I.S., 2014. Origin of Basalts in aHot Subduction Setting: petrological and Geochemical Insights from Mt. Baker, Northern Cascade Arc. J. Petrol. 55, 241–281.
Naqvi, S.M., Rogers, J.J.W., 1987. Precambrian Geology of India. Oxford University Press, New York, p. 223.
Pearce, J.A., Peate, D.W., 1995. Tectonic implications of the composition of volcanic arc magmas. Annu. Rev. Earth Planet. Sci. 23, 251–285.
Peccerillo, A., Taylor, S.R., 1976. Geochemistry of Eocene calc-alkaline volcanic rocks from the Kastamonu area, northern Turkey. Contrib. Miner. Petrol. 58, 130–143.
Perfit, M.R., Gust, D.A., Bence, A.E., Arculus, R.J., Taylor, S.R., 1980. Chemical characteristics of island arc basalts: implications for mantle sources. Chem. Geol. 30, 227–256.
Petrone, C.M., Ferrari, L., 2008. Quaternary adakite-Nb-enriched basalt association in the western Trans-Mexican Volcanic Belt: is there any slab melt evidence? Contrib. Miner. Petrol. 156, 73–86.
Petrone, C.M., Francalanci, L., Ferrari, L., Schaaf, P., Conticelli, S., 2006. The San Pedro-Cerro Grande Volcanic Complex (Nayarit, Mexico): inferences on volcanology and magma evolution. In: Siebe, C., Aguirre-Dıʻaz, G., Macıʻas, J.L. (Eds.), Neogene-Quaternary Continental Margin Volcanism: A Perspective from Mexico, vol. 402. Geological Society of America, pp. 65–68.
Poidevin, J.L., 1994. Boninite like rocks from the Paleoproterozoic greenstone belt of Bogoin, Central African Republic: geochemistry and petrogenesis. Precambr. Res. 68, 97–113.
Polat, A., Kerrich, R., 2001. Magnesian andesites, Nb-enriched basalts-andesites, and adakites from late Archean 2.7 Ga Wawa greenstone belts, Superior Province, Canada: implications for late Archean subduction zone petrogenetic processes. Contrib. Miner. Petrol. 141, 36–52.
Polat, A., Munker, C., 2004. Hf-Nd isotope evidence for contemporaneous subduction processes in the source of late Archaean arc lavas from the Superior Province, Canada. Chem. Geol. 213, 403–429.
Polat, A., Kerrich, R., 2006. Reading the geochemical fingerprints of Archean hot subduction volcanic rocks: evidence for accretion and crustal recycling in a mobile tectonic regime. Am. Geophys. Monogr. 164, 189–213.
Polat, A., Hofmann, A.W., Rosing, M.T., 2002. Boninite-like volcanic rocks in the 3.7–3.8 Ga Isua greenstone belt, West Greenland: geochemical evidence for intra-oceanic subduction zone processes in the early Earth. Chem. Geol. 184, 231–254.
Ramakrishnan, M., Vaidyanadhan, R., 2010. Geology of India, vol. 1. Geological Society of India, Bangalore, p. 556.
Rapp, R.P., Shimizu, N., Norman, M.D., Applegate, G., 1999. Reaction between slab derived melts and peridotite in the mantle wedge: experimental constraints at 3. 8 GPa. Chem. Geol. 160, 335–356.
Ray, J., Das, S., Bhattacharyya, P., 2006. Malangtoli lava of the eastern Indian shield: some aspects of major-element geochemistry and tectonic affiliation. Indian Miner. 60, 55–68.
Rogers, G., Saunders, A.D., 1989. Magnesian andesites from Mexico, Chile and the Aleutian Islands: implications for magmatism associated with ridge-trench collision. In: Crawford, A.J. (Ed.), Boninites and Related Rocks. Unwin Hyman, London, pp. 416–445.
Roy, A., Sarkar, A., 2006. Geochronological constraints on evolution of Singhbhum mobile belt and associated basic volcanics of Eastern Indian shield – comment. Gondwana Res. 9, 541–544.
Roy, A., Sarkar, A., Jeyakumar, S., Aggrawal, S.K., Ebihara, M., 2002. Mid-Proterozoic plume-related thermal event in eastern Indian Craton: evidence from trace elements, REE geochemistry and Sm-Nd isotope systematics of basic-ultrabasic intrusives from Dalma Volcanic Belt. Gondwana Res. 5, 133–146.
Saccani, E., 2015. A new method of discriminating different types of post-Archean ophiolitic basalts and their tectonic significance using Th-Nb and Ce-Dy-Yb systematic. Geosci. Front. 6, 481–501.
Saha, A.K., 1994. Crustal Evolution of Singhbhum-North Orissa, Eastern India, Memoir 27. Geological Society of India, pp. 1–341.
Saha, A.K., Ray, S.L., Sarkar, S.N., 1988. Early history of the Earth: evidence from the eastern Indian shield. In: Mukhopadhyay, D. (Ed.), Precambrian of the Eastern Indian Shield. Memoir 8.. Geological Society of India, pp. 13–37.
Sajona, F.G., Maury, R.C., Bellon, H., Cotton, J., Defant, M.J., Pubellier, M., Rangin, C., 1993. Initiation of subduction and the generation of slab melts in western and eastern Mindanao, Philippines. Geology 21, 1007–1010.
Sajona, F.G., Maury, R.C., Bellon, H., Cotton, J., Defant, M., 1996. High field strength element enrichment of Pliocene-Pleistocene island arc basalts, Zamboanga Peninsula, western Mindanao (Philippines). J. Petrol. 37, 693–726.
Santosh, M., Yang, Q.Y., Shaji, E., Tsunogae, T., Ram Mohan, M., Satyanarayanan, M., 2015. An exotic Mesoarchean microcontinent: the Coorg Block, southern India. Gondwana Res. 27, 165–195.
Sarkar, S.N., Ghosh, D., Lambert St, R.J., 1986. Rubidium–strontium and lead isotopic studies on the Soda Granites from Mosaboni, Singhbhum copper belt, E. India. Indian J. Earth Sci. 13, 101–116.
Sharma, R.S., 2009. Cratons and Fold Belts of India. Springer Verlag, Heidelberg, p. 324.
Sato, M., Shuto, K., Uematsu, M., Takahashi, T., Ayabe, M., Takanashi, K., Ishimoto, H., Kawabata, H., 2013. Origin of Late Oligocene to Middle Miocene adakitic andesites, high magnesian andesites and basalts from the back-arc margin of the SW and NE Japan arcs. J. Petrol. 54, 481–524.
Schuth, S., Gornyy, V.I., Berndt, J., Shevchenko, S.S., Sergeev, S.A., Karpuzov, A.F., Mansfeldt, T., 2012. Early Proterozoic U–Pb zircon ages from basement gneiss at the Solovetsky Archipelago, White Sea, Russia. Int. J. Geosci. 3, 289–296.

Sengupta, S., Bandopadhyay, P.K., Van den Hul, H.J., Chattopadhyay, B., 1984. Arkasani granophyre: Proterozoic intraplate acid magmatic activity in the Singhbhum craton, eastern India. Neues Jahrbuch fur Mineralogie - Abhandlungen 148, 328–343.
Shimoda, G., Tatsumi, Y., Nohda, S., 1998. Setouchi high-Mg andesites revisited: geochemical evidence for melting of subducting sediments. Earth Planet. Sci. Lett. 160, 479–492.
Shinjo, R., 1999. Geochemistry of high Mg andesites and the tectonic evolution of the Okinawa trough-Ryuku arc system. Chem. Geol. 157, 69–88.
Shirey, S.B., Hanson, G.N., 1984. Mantle-derived Arcaean monzodiorites and trachyandesites. Nature 310, 222–224.
Shuto, K., Sato, M., Kawabata, H., Osanai, Y., Nakano, N., Yashima, R., 2013. Petrogenesis of Middle Miocene primitive basalt, andesite and garnet-bearing adakitic rhyodacite from the Ryozen Formation: implications for the tectono-magmatic evolution of the NE Japan arc. J. Petrol. 54, 2581–2596.
Singh, R.M., Manikyamba, C., Ray, Jyotisankar., Ganguly, S., Santosh, M., Saha, A., Rambabu, S., Sawnt, S.S., 2016. Major, trace and Platinum Group Element (PGE) geochemistry of Archean Iron Ore Group and Proterooic Malangtoli metavolcanic rocks of Singhbhum Craton, eastern India: inferences on mantle melting and sulphur saturation history. Ore Geol. Rev. 72, 1263–1289.
Smithies, R.H., 2002. Archean boninite like rocks in intracratonic setting. Earth Planet. Sci. Lett. 197, 19–34.
Smithies, R.H., Champion, D.C., 2000. The Archaean high-Mg diorite suite: links to tonalite-trondhjemite-granodiorite magmatism and implications for early Archaean crustal growth. J. Petrol. 41, 1653–1671.
Spandler, C., Pirard, C., 2013. Element recycling from subducting slab to arc crust: A review. Lithos 170–171, 208–223.
Stern, C.R., Kilian, R., 1996. Role of the subducted slab, mantle wedge and continental crust in the generation of adakites from the Austral Volcanic zone. Contrib. Miner. Petrol. 123, 263–281.
Stern, R.J., Lin, P.-N., Morris, J.D., Jackson, M.C., Fryer, P., Bloomer, S.H., Ito, E., 1990. Enriched back-arc basin basalts from the northern Mariana Trough: implications for the magmatic evolution of back-arc basins. Earth Planet. Sci. Lett. 100, 210–225.
Sun, S.S., McDonough, W.F., 1989. Chemical and isotopic systematics of oceanic basalts, implications for mantle composition and processes. In: Saunders, A.D., Norry, M.J. (Eds.), Magmatism in the Ocean Basins. Geological Society of London Special Publication 42. Blackwell Scientific Publication, UK, pp. 313–345.
Tatsumi, Y., 2005. The subduction factory: how it operates in evolving earth. GSA Today 15 (7), 4–10.
Tatsumi, Y., 2006. High-Mg andesites in the Setouchi volcanic belt, southwestern Japan: analogy to Archean magmatism and continental crust formation? Annu. Rev. Earth Planet. Sci. 34, 467–499.
Tatsumi, Y., Ishizuka, K., 1982. High magnesian andesite and basalt from Shodo-shima island, southwest Japan, and their bearing on the genesis of calc-alkaline andesites. Lithos 15, 161–172.
van Keken, P.E., Hacker, B.R., Syracuse, E.M., Abers, G.A., 2011. Subduction factory: 4. Depth-dependent flux of H_2O from subduction slabs worldwide. J. Geophys. Res. 116, 1–15.
Viruete, J.E., Contreras, F., Stein, G., Urien, P., Joubert, M., Perez-Estaun, A., Friedman, R., Ullrich, T., 2007. Magmatic relationships and ages between adakites, magnesian andesites and Nb-enriched basalt-andesites from Hispaniola: record of a major change in the Caribbean island arc magma sources. Lithos 99, 151–177.
Wang, L.L., Chung, S.L., Chen, C.H., 2002. Geochemical constraints on the petrogenesis of high-Mg-basaltic andesites from the Northern Taiwan Volcanic Zone. Chem. Geol. 182, 513–528.
Wang, Q., Wyman, D.A., Zhao, Z.H., Xu, J.F., Zheng, H.B., Xiong, X.L., Dai, D.X., Li, H.C., Chu, Z.Y., 2007. Petogenesis of Carboniferous adakites and Nb-enriched arc basalts in the Alataw area, northern Tianshan range (western China): implications for Phanerozoic crustal growth in the central Asia orogenic belt. Chem. Geol. 236, 42–64.
Wang, Q., Wymen, Derek A., Xu, J., Wan, Y., Li, Q., Zi, F., Jiang, Z., Qui, H., Chu, Z., Zhao, Z., Dong, Y., 2008. Triassic Nb-enriched basalts, magnesian andesites, and adakites of the Qiantang terrane (Central Tibet): evidence for metasomatism by slab-derived melts in the mantle wedge. Contrib. Miner. Petrol. 155, 473–490.
Weaver, B.L., 1990. Geochemistry of highly-undersaturated ocean island basalt suites from the South Atlantic Ocean: Fernando de Noronha and Trindade Islands. Contrib. Miner. Petrol. 105, 502–515.
Wyman, D.A., Ayer, J.A., Devaney, J.R., 2000. Niobium-enriched basalts from the Wabigoon subprovince, Canada: evidence for adakitic metasomatism above an Archaean subduction zone. Earth Planet. Sci. Lett. 179, 21–30.
Xiong, X., Keppler, H., Audetat, A., Ni, H., Sun, W., Li, Y., 2011. Partitioning of Nb and Ta between rutile and felsic melt and the fractionation of Nb/Ta during partial melting of hydrous metabasalt. Geochim. Cosmochim. Acta 75, 1673–1692.
Xu, J.F., Wang, Q., Yu, X.Y., 2000. Geochemistry of high-Mg andesites and adakitic andesites from the Sanchazi block of the Mian-Lue ophiolitic melange in the Qinling Mountains, central China: evidence of partial melting of the subducted Paleo-Tethyan crust. Geochem. J. 34, 359–377.
Yang, Q.Y., Santosh, M., Collins, A.S., Teng, X.M., 2016. Microblock amalgamation in the North China Craton: evidence from Neoarchaean magmatic suite in the western margin of the Jiaoliao Block. Gondwana Res. 31, 96–123.
Yogodzinski, G.M., Kay, R.W., Volynets, O.N., Koloskov, A.V., Kay, S.M., 1995. Magnesian andesite in the western Aleutian Komandorsky region: implication for slab melting and processes in the mantle wedge. Bull. Geol. Soc. Am. 107, 505–519.
Zhao, J.J., Zhou, M.F., 2007. Geochemistry of Neoproterozoic mafic intrusions in the Panzhihua district (Sichuan Province, SW China): implications for subduction related metasomatism in the upper mantle. Precambr. Res. 152, 27–47.
Zhang, H., Niu, H., Sato, H., Yu, X., Shan, Q., Zhang, B., Ito, J., Nagao, T., 2005. Late Palaeozoic adakites and Nb-enriched basalts from northern Xinjiang northwest China: evidence for the southward subduction of the Paleo-Asian Oceanic plate. Island Arc 14, 55–68.